A physiologically based pharmacokinetic (PBPK) model exploring the blood-milk barrier in lactating species - A case study with oxytetracycline administered to dairy cows and goats

Jennifer Tardiveau, Lerica Leroux-Pullen, Ronette Gehring, Gaël Touchais, Marie-Pierre Chotard, Hélène Mirfendereski, Carine Paraud, Matthieu Jacobs, Reynald Magnier, Michel Laurentie, et al.

A Physiologically Based Pharmacokinetic (PBPK) Model Exploring the Blood-Milk Barrier in Lactating Species

-A case study with oxytetracycline administered to dairy cows and goats-

Jennifer Tardiveau[1,2], Lerica LeRoux-Pullen[3], Ronette Gehring[3], Gaël Touchais[4], Marie Pierre Chotard-Soutif[4], Hélène Mirfendereski[1,5], Carine Paraud[6], Matthieu Jacobs[7#], Reynald Magnier[7], Michel Laurentie[4], William Couet[1,2,5], Sandrine Marchand[1,2,5], Alexis Viel[4$], Nicolas Grégoire[1,2,5$*]

[1] INSERM** U1070, 1 rue Georges Bonnet, 86022 Poitiers Cedex, France

[2]Université de Poitiers, UFR de Médecine Pharmacie, 6 rue de la Milétrie 86073 Poitiers Cedex, France

[3]Department of Population Health Sciences: IRAS Veterinary and Comparative Pharmacology, Faculty of Veterinary Medicine, Utrecht University, Yalelaan 104, 3508 TD Utrecht, The Netherlands

[4]ANSES, Laboratoire de Fougères, 10B rue Claude Bourgelat, Bioagropolis, Javené 35306 Fougères, France

[5]CHU de Poitiers, département de toxicologie et pharmacocinétique, 2 rue de la Milétrie 86073 Poitiers Cedex, France

[6]ANSES, Laboratoire de Ploufragan-Plouzané-Niort, site de Niort, 60 rue de Pied de Fond 79024, Niort, France

[7]Ceva Santé Animale, Libourne I&D Center, 10 Avenue de la Ballastière, 33500 Libourne, France

[#]Present address: Servier, Quantitative Pharmacology department, 25 rue Eugène Vignat, 45000 Orléans, France

[$]These authors contributed equally to this work

*To whom correspondence should be addressed: nicolas.gregoire@univ-poitiers.fr ; Address: 1 rue Georges Bonnet, 86022 Poitiers Cedex, France.

** National Institute of Health and Medical Research

Abbreviations: AUC: area under the time concentration curve; BLQ: below the lower limit of quantification; C_{max}: maximal concentration; CV: coefficient of variation; EW: extracellular water; GSA: global sensitivity analysis; IIV: inter-individual variability; IM: intramuscular; IMI: inter-milking interval; IV: intravenous; IW: intracellular water; LLOQ: lower limit of quantification; MAPE: mean absolute percentage error; MP: milk to plasma ratio; MRL: maximum residue limit; OTC: oxytetracycline; PBPK: physiologically based pharmacokinetic; PK: pharmacokinetic; PI: prediction interval; R^2: coefficient of determination; RV: residual error; SAEM: stochastic approximation expectation-maximization; T_{max}: time of the maximal concentration; ULOQ: upper limit of quantification; VASC: vascular space; VPC: visual predictive check; WHO: World Health Organization; WP: withdrawal period.

1. Introduction

Understanding the passage of drugs into milk is important in order to manage residues in foodstuffs of animal origin thus optimizing the withdrawal period for both food safety (limiting risks for consumers), and for economic reasons such as milk being discarded where drug residues are below the maximum residue limits (MRLs). To address these issues, it is essential to accurately predict the concentration of a drug in milk over time.

After administration, drugs are absorbed, distributed, and eliminated, following pharmacokinetic (PK) processes that depend on the physico-chemical properties of the compound and the physiology of the animal. Their distribution in milk depends on the same PK processes which are adapted to the particularities of the udder physiology and the composition of the milk. Milk is an emulsion of fat globules in an aqueous medium containing soluble proteins, casein, and minerals.

The distribution of a compound in the different milk fractions (*i.e.*, cream, curd, whey) depends on factors specific to the compound, such as its lipophilicity or ionization, as well as factors specific to the milk, such as its composition or volume (Hotham and Hotham, 2015; Ozdemir, 2018; Whittem, 2012).

Physiologically based pharmacokinetic (PBPK) models integrate the physico-chemical properties of drugs and the physiological parameters of species (Lin *et al*., 2016). In particular, these models make predicting compound concentrations in various fluids and tissues after different dosing regimens possible. They can be of particular interest for predicting the excretion of compounds into the milk of various species.

In recent years, several PBPK models have been developed for use in veterinary medicine. Most of them are used to predict tissues residues and withdrawal periods in farm animals for food safety assessment (Lautz *et al*, 2019). Few PBPK models describing the excretion of drugs into milk exist for dairy cows (Leavens *et al*, 2014; Li *et al*, 2018; Woodward and Whittem, 2019). At present, there are no models for dairy goats or ewes.

Moreover, some essential factors affecting distribution in milk are not taken into account in the currently published models. For instance, excretion into milk was modeled as a

simple, first order elimination from plasma (Leavens *et al*, 2014) and did not account for udder size, composition, and perfusion, or variation in the volume of milk produced and milking frequency (Abduljalil *et al*, 2021). Other models are more physiological and describe the structure of the udder (Li *et al*, 2018; Woodward and Whittem, 2019), but they do not consider permeability-limited passive diffusion and active transport within mammary cells and they do not describe the distribution in the different milk fractions or the binding of molecules to the different milk constituents.

Oxytetracycline (OTC) is a broad-spectrum antibiotic from the tetracycline family. It is widely used in veterinary medicine to treat infectious diseases (Craigmill *et al*, 2000). OTC PK is well-known in multiple veterinary species (Aktas and Yarsan, 2017; Craigmill, 2003; Nouws *et al*, 1985b; Rule *et al*, 2001). Briefly, it has a good bioavailability in cattle after intramuscular (IM) injection and, is distributed to most tissues and fluids such as milk. It is mainly excreted unchanged in the urine by glomerular filtration and tubular secretion and, to a lesser extent, it is excreted unchanged in bile (Nouws *et al*, 1985b). Its off-label use led to various adverse effects at higher doses (in the kidneys and liver) as well as violative residues in edible tissues (Riad *et al*, 2021). The published OTC PK studies have resulted in the development of PBPK models of OTC in non-lactating food animal species such as cattle (Achenbach, 1995), sheep (Craigmill, 2003), and goats (Riad *et al*, 2021) as well as in dogs (Lin *et al*, 2015) and salmon (Law, 1999), for different formulations. To the knowledge of the authors of this study, however, there is no PBPK model to predict OTC distribution in milk.

The objective of this study has been to develop a PBPK model to describe the excretion of OTC in cow and goat milk. To be able to complete this model at a later stage and come up with a generic model that can be used for other drugs and/or species, the development a detailed model for OTC was attempted. Therefore, the development of a rather detailed PBPK model, which could be adapted to the data available for these different compounds and species was chosen.

The generic PBPK model thus developed was then applied in a case study to predict OTC concentrations in cow and goat milk.

2. Materials and methods

OTC plasma and milk concentrations in cows and goats were obtained experimentally prior to the development of the PBPK model in order to calibrate and/or validate the model. *In vitro* permeability studies, in a Parallel Artificial Membrane Permeability Assay (PAMPA), were performed in order to calibrate the (transcellular) passive diffusion of OTC from plasma to milk. In the following paragraphs, the experimental studies (properties of OTC, animal study, *in vitro* experimentation, and analytical methods) will be presented first. Then, the development of the PBPK model (the global structure, the udder, and milk model). And finally, the calibration and validation of the model will be elaborated.

2.1. Experimental studies

2.1.1. Chemicals

(All chemicals used in analytical assays were of analytical grade)

OTC in hydrochloride form (Terramycine solution injectable®; Zoetis, Malakoff, France) was used for the *in-vivo* experiments. Its octanol-water partition coefficient (logP) and its pKa were determined from Chemicalize ("Chemicalize - Instant Cheminformatics Solutions," n.d.). The logP of OTC was estimated to be -4.54.

OTC has several chemical groups which, depending on the pH, may have an electric charge. The two main groups of OTC that can have an electric charge in physiological pH (~7) have an acid pKa of 7.25 and a basic pKa of 5.80, respectively. According to Rodgers and Rowland's publications (Rodgers *et al*, 2005; Rodgers and Rowland, 2006), OTC was considered as a zwitterion of group 2 since it has no basic pKa $\geq$ 7. The ionization ratios of OTC in the different media were calculated from the equations reported by Rodgers and Rowland (see Equation 1) (Rodgers *et al*, 2005; Rodgers and Rowland, 2006).

$$Ionisation\ ratio = 1 + 10^{pKa_{Base} - pH_i} + 10^{pH_i - pKa_{Acid}} \quad (1)$$

where pH_i is the pH of the i^{th} media, and pKa_{Base} and pKa_{Acid}, the basic and acid pKa of OTC, respectively.

130

131 2.1.2. Animals

132 Six (6) Prim' Holstein cows along with five (5) Alpine goats and one (1) crossbred goat
133 were included in the study which had been approved by the Animal Research Ethics Committee
134 (APAPHIS n° 19369-2019022111373719). Each animal received a drug-free diet and water *ad*
135 *libitum*. All animals were free of clinical mastitis. Goats and cows were milked twice daily:
136 at 8h and 16h--meaning a milking interval of 8 hours during the day and of 16 hours during
137 the night--by a milking unit and a milking robot, respectively. Each animal received a single
138 dose of OTC conventional formulation at 10 $mg.kg^{-1}$ by intramuscular (IM) route in the neck,
139 at several injection points. Blood samples were taken from jugular vein by venipuncture at
140 0.5, 1, 2, 3, 4, 6, and 8-hours post-administration and then, twice daily (in the morning and
141 evening, at the same time as milking) until the 4^{th} day after the administration. Within 30 min
142 after sampling, blood samples were centrifuged at 3500 rpm at room temperature for 10
143 minutes and plasma was collected. Milk samples (about 20 mL) mixed from all the teats (4
144 for cows, 2 for goats) were taken at each milking starting at 8 hours post-administration and
145 continued up to 5 days. The volumes of milk collected were measured at each milking. The
146 butyrous and protein rates were quantified once for each individual's milk at the beginning of
147 the experiment **(see the demographic characteristics of the animals are presented in the**
148 **Table S1 of the supplementary materials)**.

149

150 Blank samples of blood and milk (without drug) were collected before administration. All
151 samples were frozen and stored at -20°C and protected from light until analysis.

152

153 2.1.3. PAMPA experiments

154 The PAMPA, as first described by Kansy *et al*, was used as an *in vitro* model of passive
155 transcellular permeation (Kansy *et al*, 1998). PAMPA was performed using the Corning®
156 Gentest™ Pre-coated PAMPA Plate System (Corning, NY 14831, USA). This plate system
157 consisted of pre-coated inserts of structured layers of phospholipids, composed of hexadecane
158 in hexane (5 % v/v). The PAMPA protocol published by Corning® (Chen *et al*, 2008), with
159 minor adaptations, was performed as follows: A stock solution of 10mM OTC in DMSO was
160 prepared and further diluted in PBS to a final concentration of 200 µM (100 mg/L). A
161 volume of 300 µL of solution was added to each well of the receiver plate and 200 µL of PBS

were added to the pre coated filter plate's wells. The plate was then incubated for four hours at room temperature, without agitation. After the incubation period, two (2)-100 µL samples were collected from each well and stored at -80°C until analysis.

After analytical analysis of the samples, the apparent permeability of OTC over the synthetic membrane was calculated using the following formula (Equation 2) (Shanler *et al*, 2021):

$$P_{app} = \frac{-\ln\left(\frac{1-C_A(t)}{Ceq}\right)}{A\times\left(\frac{1}{V_D}+\frac{1}{V_A}\right)\times t} \quad (2)$$

with $C_{eq} = \frac{C_D(t)\times V_D + C_A(t)\times V_A}{V_D+V_A}$

where A is the filter area (0.3 cm^2), V_D is the donor well volume (0.3 mL), V_A is the acceptor well volume (0.2 mL), t is the incubation time (in seconds), $C_A(t)$ is the compound concentration in acceptor well at time t, $C_D(t)$ is the compound concentration in donor well at time t, C_{eq} corresponds to the concentration at equilibrium.

2.1.4. Analytical Methods

Plasma samples were assayed by Shimadzu high-performance liquid chromatography system (Shimadzu, SBM-20A, Marne la Vallée, France) coupled with an ultraviolet detector (Shimadzu, SDP-20A). A volume of 100 µL of plasma sample was mixed with 50 µL of internal standard solution: demeclocycline hydrochloride at 12 µg/ml in trichloroacetic acid 10% and centrifuged for 10 min at 14000 rpm at about 7°C. Supernate was transferred into a vial with a polypropylene insert and 20 µL of the solution were injected into the chromatographic system. The analytical column was a Luna Omega Polar C_{18} (150 * 2.1 mm, 5 µm), fitted with a Luna Omega C_{18} precolumn (4 x 2.0mm) (Phenomenex, Torrance, California, USA). The mobile phase was composed of KH_2PO_4 solution at 0.025 mol/L and pH 3.0 (adjusted with phosphoric acid), and an acetonitrile solution (90:10 [vol/vol]) and was delivered isocratically at 0.3 mL/min. Rinsing of the needle with 100 µL of a methanol/water/isopropanol/acetonitrile mixture (25:25:25:25) was done between each injection and repeated rinsing of the system with ACN and HPLC grade water in gradient mode was used at the end of the run. The UV detection was at 355 nm. The retention time

was 8 min for OTC and 14 min for the internal standard. The lower and upper limits of quantification (LLOQ and ULOQ) of the method were 0.05 µg/mL and 15 µg/mL, respectively. The trueness and precision were characterized at five concentration levels (0.05, 0.2, 6, 10, and 15 µg/ml) with a relative bias between -7.1% and 5.8% for goats; -5.1% and 10.2% for cows; a repeatability between 0.1% and 2.0% for goats; 0.6% and 3.1% for cows; and an intermediary precision between 1.5% and 3.0% for goats; 1.0% and 5.4% for cows.

The analytical method used to assay PAMPA samples in PBS was a modified version of the method in plasma. The same sample preparation method and chromatographic conditions were used as for plasma. The difference being the mathematical function for calibration which was quadratic instead of linear due to a slight flattening of the curve at high concentrations.

Milk samples were assayed by LC-MS/MS. Two (2) g of milk sample were mixed with 1 mL of water (HPLC grade). A volume of 200 µL of internal standard solution, demeclocyclin hydrochloride at 1 µg/ml was added, and the mixture was vortexed and left for at least 10 minutes away the light. Extraction was made by adding 10 mL of Mac Ilvaine/EDTA buffer, vortexed during 30 seconds, mixed with a rotary stirrer at 100 rpm for 10 min, and centrifuged 10 min at 14000 g at 4°C. Deproteination was made by adding 1 mL of TCA at 1 g/mL, vortexed, frozen for 15 min and centrifuged 5 min at 14000 g. Purification was made by solid phase extraction (SPE) using Bond Elut C18 cartridges (200 mg/3cc - Agilent Technologies) and elution by oxalic acid solution at 0.01 mol/L before filtration with 0.45 µm filter. Five (5) µL were injected into the chromatographic system composed of Quadrupole tandem mass spectrometer: Type TSQ Vantage (Thermo Scientific) with data acquisition station: Xcalibur version 2.2.SP1. The analytical column was a Kinetex® Biphenyl C_{18} (100 x 2,1 mm, 2.6 µm) (Phenomenex, Torrance, California, USA). The mobile phase A was a formic acid solution at 0.2% in water, and mobile phase B was a formic acid solution at 0.2% in methanol. The gradient for mobile phase B was set at 5%, 98%, and 5% at 0.01, 5, and 6.1 min, respectively, with a flow rate of 0.35 mL/min. Heated-electrospray ionization (H-ESI) in positive mode was used for the detection of OTC. Ions were analyzed in the multiple reaction monitoring, and the following transitions were inspected: 461.1 *m/z* → $[M+H]^+$ > 426.16 *m/z* and 465.1 *m/z* → $[M+H]^+$ > 448.10 *m/z* for OTC and IS, respectively. The ion used for quantification is the one with the m/z of 426.16 for OTC and the one with the m/z of 448.10 for IS. The retention time was 4.4 min for OTC and 4.8 min for the internal

standard. The lower and upper limits of quantification of the method were 20 µg/kg and 1000 µg/kg (0.2 to 10 times the MRL), respectively. The trueness and precision were characterized at six (6) concentration levels (20, 40, 100, 300, 500, and 1000 µg/kg) with a relative bias between -0.1% and 1.8% for goats; -3.2% and 3.7% for cows; a repeatability between 0.5% and 1.7% for goats; 1.0% and 1.6% for cows; and an intermediary precision between 3.3% and 4.8% for goats; 1.0% and 4.8% for cows.

2.2. Global PBPK Model Structure

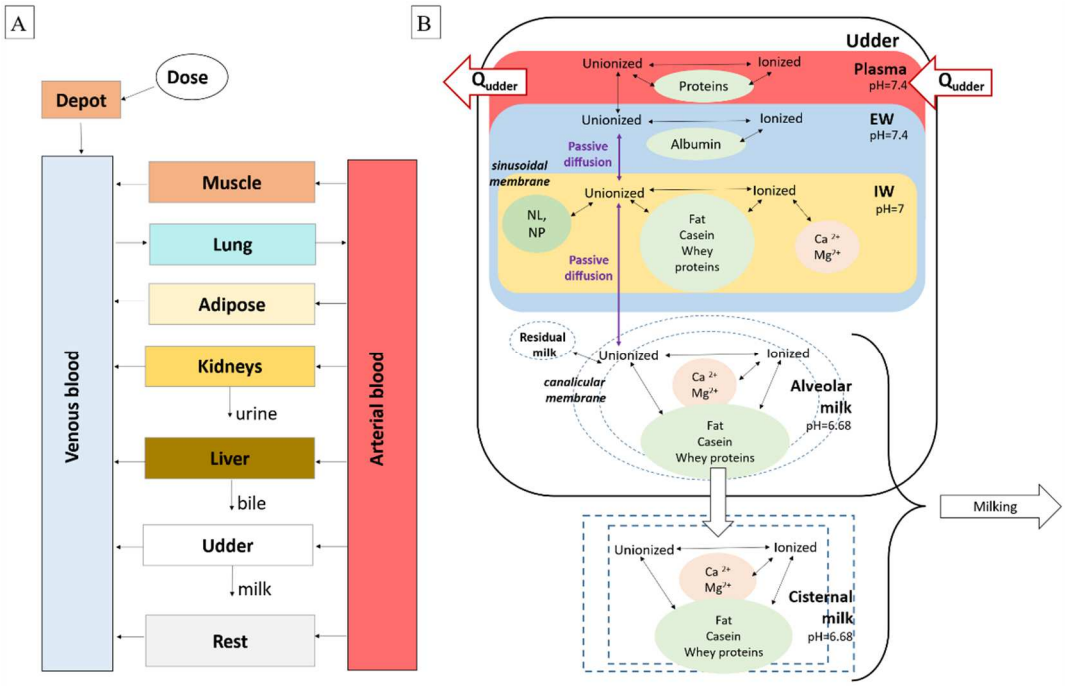

Figure 1: (A) Schematic diagram of the whole PBPK model to explore the blood-milk barrier in lactating species. Intramuscular (IM) administration was considered through the IM injection site compartment. The "rest" compartment was composed of remaining organs with no specific interest. (B) Schematic representation of the udder sub-compartments. The udder is described as a multi-compartmental, permeability-limited model, composed of an interstitial space consisting of extracellular water (EW), an intracellular water (IW) and the milk which is produced in the udder alveolar cells (alveolar milk) and stored in the cistern (cisternal milk). Passive diffusion between sub-compartments and binding to several proteins (*i.e.,* casein, whey proteins), lipids (NL for neutral lipids, NP for neutral phospholipids and ions (Ca^{2+} for calcium, Mg^{2+} for magnesium) were considered.

The PBPK model was composed of ten compartments corresponding to the main body organs and tissues (lung, adipose, muscle), blood compartments (arterial, venous), absorption compartment (IM injection site), excretory organs (kidneys, liver), tissue of interest (udder: see section 2.3), and a lumping compartment for the rest of the body (Figure 1A). All compartments interconnected by blood flows, with the exception of the IM injection site compartment, were defined by volume and blood flow rates obtained from published experimental studies with healthy animals for each species **(see Table S2 in supplementary materials)** (Lin *et al*, 2020); (Li *et al*, 2021); (Jackson and Cockcroft, 2002); (Upton, 2008); (Lin *et al*, 2016); (Maltz *et al*, 1984); (Ji *et al*, 2017); (Lautz *et al*, 2020); (Williams *et al*, 2007); (McCutcheon *et al*, 1993); (Rodgers *et al*, 2005). The distribution of OTC from the plasma to the tissues was considered as perfusion limited, consistent with previous PBPK models of OTC in cattle, sheep and goats (Craigmill, 2003; Riad *et al*, 2021). A more detailed model was developed for the udder, taking into account the permeability data generated *in vitro* (see section 2.1.3).

The IM absorption was modelled by a single IM injection site compartment connected to the venous blood compartment by an intramuscular absorption rate (k_{IM}) (Equation 3).

$$\frac{dA_{injection}}{dt} = -k_{IM} \times A_{injection} \quad (3)$$

with $A_{injection}$ the drug quantity in the IM injection site compartment calculated as $A_{injection} = dose \times F_{IM}(\%)$ and F_{IM} as the intramuscular bioavailability. For each species k_{IM} value was estimated by fitting the PBPK model with experimental plasma data from the current study (see section 2.4), whereas F_{IM} values were obtained in the literature (Nouws *et al*, 1985b; Rule *et al*, 2001) (see Table 1).

Drug partition between blood and plasma was based on the blood to plasma ratio (BP), (**see details in section 2.2.2 of the supplementary materials**) and used to convert plasma concentrations to blood concentrations.

Drug distribution was dependent on the tissue to plasma partition coefficient (k_{tissue}) for each tissue, defined as the ratio between total tissue drug concentration and total plasma concentration (Yau *et al*, 2020). The k_{tissue} values were obtained in the literature from OTC tissue and serum residues in sheep (Craigmill, 2003), with the exception of the lungs which were estimated from residues data in cattle (Achenbach, 1995) (**see details in section 2.2.3 of the supplementary material**) (see Table 1). For the lumping compartment, the partition coefficient (k_{rest}) was calculated as the weighted mean of the partition coefficients of the lumped organs (Equation 4) (Nestorov *et al*, 1998). As partition coefficients were missing for these lumped tissues, the partition coefficient of the muscle was used for poorly perfused tissues (brain and gastrointestinal tracts) and the partition coefficient of the kidneys was used for richly perfused tissues (bones, carcass, heart, pancreas, spleen) (Lin *et al*, 2015).

$$k_{rest} = \frac{k_{muscle} \times V_{poorly_{perfused}} + k_{kidneys} \times V_{richly_{perfused}}}{V_{poorly_{perfused}} + V_{richly_{perfused}}} \quad (4)$$

where $V_{poorly_{perfused}} = V_{GItract} + V_{Intestines} + V_{Brain}$

and $V_{richly_{perfused}} = V_{Bones} + V_{Carcass} + V_{Heart} + V_{Pancreas} + V_{Spleen}$

With k_{muscle} and $k_{kidneys}$ as the tissue to plasma partition coefficient of the muscle and kidneys, and V_{tissue} as the volume of tissue.

Distribution of drug in the non-eliminating organs is described using the following equation (Equation 5):

$$\frac{dA_{tissue}}{dt} = Q_{tissue} \times \left(C_{art} - \frac{C_{tissue}}{k_{tissue}} \times BP\right) \quad (5)$$

with A_{tissue} the amount of drug in tissue, Q_{tissue} the tissue blood flow rate, C_{art} and C_{tissue} the concentration of drug in arterial blood and tissue, respectively, and BP the blood to plasma ratio and k_{tissue} the tissue to plasma partition coefficient.

OTC total plasma clearance values (CL_{plasma}) for both species was obtained by averaging values reported in several articles for cattle (Craigmill *et al*, 2004; Nouws *et al*, 1985b), and goats (Aktas and Yarsan, 2017; Rule *et al*, 2001) (see Table 1). These clearances were split between renal and hepatic clearances only based on the unchanged excreted fraction in urine ($fe_{kidneys}$) reported in the literature (Nouws *et al*, 1985b) (see Table 1). The excretion clearance in milk was considered independently of the systemic clearance (see section 2.3). The differential equation describing the variation in the amount of OTC in the eliminating organs (liver and kidney) is as follows (Equation 6):

$$\frac{dA_{tissue}}{dt} = Q_{tissue} \times \left(C_{art} - \frac{C_{tissue}}{K_{tissue}} \times BP\right) - Q_{tissue} \times ER_{tissue} \times C_{art} \quad (6)$$

with ER_{tissue} the extraction ratio of the corresponding tissue.

The extraction ratio of both organs were calculated based on CL_{plasma} and $fe_{kidneys}$ as follows (Equations 7 and 8):

298

$$ER_{blood,kidneys} = \frac{CL_{plasma} \times fe_{kidneys}}{BP \times Q_{kidneys}} \quad (7)$$

$$ER_{blood,liver} = \frac{CL_{plasma} \times (1 - fe_{kidney})}{BP \times Q_{liver}} \quad (8)$$

299

300

301 2.3. Udder and Milk Model

302 The udder is described as a multi-compartment, permeability-limited model (Figure 1B).
303 It is composed of a vascular space (VASC), an interstitial space consisting of extracellular
304 water (EW), an intracellular water (IW) of mammary epithelial secretory cells, and 2
305 compartments containing the milk. Between each milking, milk components were produced
306 within the epithelial secretory cells (alveolar milk), then passed the canalicular membrane and
307 reaching the cistern (cisternal milk) through the ducts.

308

309 This study hypothesized that only the unbound and unionized form of the drug diffused
310 passively between EW and IW and between IW and alveolar milk. The fraction of ionized
311 OTC in each sub-compartment was calculated based on the pH of these compartments and the
312 pKas of OTC, and the diffusion rate between EW and IW and between IW and alveolar milk
313 was estimated based on *in vitro* PAMPA results. In IW as in milk, OTC is presumed to be
314 distributed between the fat and aqueous fractions and to bind to casein, whey proteins, ionized
315 calcium, and magnesium.

316

317 2.3.1. Permeability

318 Passive diffusion, the main mechanism of OTC distribution into milk, was assessed by
319 PAMPA experiments (Fujikawa *et al*, 2005) as detailed in section 2.1.3. This synthetic
320 membrane permitted an estimation of the permeability (P_{app} in cm/s) (see Table 1)
321 representing transcellular diffusion that could then be applied to sinusoidal and canalicular
322 membranes. P_{app} was converted to passive milk clearance (CL_{diff} in L/h) according to the
323 following equation (Badhan *et al*, 2014) (Equation 9):

$$CL_{diff} = P_{app} \times SA \times Tissue\ weight \quad (9)$$

where SA represented *in vivo* endothelial surface area (cm²/g) and tissue weight represented the weight of the udder (g).

SA was not found in the literature for the udders of cows or goats; therefore, it was calculated considering the cylindrical structure of capillary from geometric formula (Ng and Hungerbühler, 2013) (**see section 2.3.1 of the supplementary materials for calculation details**).

2.3.2. Extracellular water

In both the EW and the VASC, the pH was considered to be 7.4 (Rodgers *et al*, 2005) (see Table 1), thus supposing instantaneous equilibrium in both spaces. The ratio between the total EW concentration and the total blood concentration in the tissue vascular space ($K_{EW/B}$) was used, allowing only one differential equation to determine the concentrations of OTC in VASC and EW (Jamei *et al*, 2014).

In addition, OTC should bind to albumin in EW. Albumin concentration in EW was found in the literature (Vestweber and Al-Ani, 1984) (see Table 1) and its affinity constant for OTC was calculated based on the unbound fraction in plasma (**see section 2.3.2.1 of the supplementary materials, equation S20**) (Rodgers and Rowland, 2006).

The variations of the amount of drug in the EW (A_{EW}) is described by the following equation (Equation 10):

$$\frac{dA_{EW}}{dt} = Q_{udder} \times C_{art} - Q_{udder} \times \frac{Cu_{EW}}{fu_{EW}} \times \frac{1}{\frac{K_{EW}}{B}} + CL_{diff,sin} \times \left(\frac{Cu_{IW}}{X} - \frac{Cu_{EW}}{Y}\right) \quad (10)$$

with

$$Cu_{EW} = \frac{A_{EW}}{V_{EW,eff}} \times fu_{EW}\ ; \qquad V_{EW,eff} = V_{EW} + \frac{V_{VASC}}{K_{\frac{EW}{B}}}\ ;$$

$$V_{EW} = f_{EW} \times V_{udder}\ ; \qquad V_{VASC} = f_{VASC} \times V_{udder}$$

where fu_{EW} is the unbound EW fraction, X and Y are the ionization ratios of OTC in IW and EW, respectively; $K_{EW/B}$ is the quotient of total EW concentration and the total blood concentration in the tissue vascular space (VASC); $CL_{diff,sin}$ is the clearance pertaining passive diffusion of drug across the sinusoidal membrane; Cu_{EW} is the unbound concentration in EW; Cu_{IW} is the unbound concentration in IW; f_{vasc} and f_{EW} are vascular and EW fractions, $V_{EW,eff}$ is the volume of effective extracellular space which is a combination of EW and VASC; V_{EW} ,V_{VASC} and V_{udder} are EW, vascular and udder volumes, respectively.

(Details for calculations of X, Y, fu_{EW} and $K_{EW/B}$ were presented in section 2.3.2 of the supplementary materials)

2.3.3. Intracellular water

In IW the pH was considered to be 7.0 (Rodgers *et al*, 2005) (see Table 1). Unionized OTC is assumed to bind to neutral lipids and phospholipids. The concentration of neutral lipids and phospholipids were fixed based on available information in the literature (Kinsella and McCarthy, 1968) (Larson, 1978). Their OTC affinity constants were calculated based on the drug lipophilicity (logP) and ionization rate in IW (X) following Rodgers and Rowland's equations (Rodgers *et al*, 2005; Rodgers and Rowland, 2006) (**see section 2.3.2.2 of the supplementary material**).

In addition, the IW compartment should contain the same components as milk, (*i.e.,* fat, casein, whey proteins [lactalbumin and lactoglobulin] and ionized calcium and magnesium). OTC should be distributed and bind to these components in IW as in milk.

The concentration of milk fat, casein, and whey proteins in IW were assumed to be identical to those in milk and are described in section 2.3.4.2. The concentration of ionized magnesium in IW was found in the literature (Martens and Stumpff, 2019). The

concentration of ionized calcium in IW was calculated based on the total concentration of calcium in IW (Neville and Watters, 1983), and the free calcium fraction in IW that was supposed to be the same as in milk (7%, see section 2.3.4.2). Calculations of their OTC affinity constants are detailed in section 2.3.4.2.

The variation of the amount of drug in the IW (A_{IW}) was described by the following equation (Equation 11):

$$\frac{dA_{IW}}{dt} = CL_{diff,sin} \times \left(\frac{Cu_{EW}}{Y} - \frac{Cu_{IW}}{X}\right) + CL_{diff,can} \times \left(\frac{Cu_{alveolar\ milk}}{Z} - \frac{Cu_{IW}}{X}\right) \quad (11)$$

with

$$Cu_{IW} = \frac{A_{IW}}{V_{IW}} \times fu_{IW} \; ; V_{IW} = f_{IW} \times V_{udder}$$

where fu_{IW} is the unbound IW fraction; Z is the ionization ratio of OTC in milk; $CL_{diff,can}$ is the passive diffusion of drug across the canalicular membrane; f_{IW} is the intracellular water fraction; V_{IW} is the volume of udder intracellular water; and $Cu_{alveolar\ milk}$ is the unbound concentration in alveolar milk space.

(Details for the calculations of Z and fu_{IW} are presented in section 2.3.2.2 of the supplementary materials)

2.3.4. Milk

2.3.4.1. Production of milk

Milk is produced by the mammary epithelial secretory cells, exported into the alveolar lumen, and transported by the ducts to the cistern where it is stored. The volume of milk contained in the udder ($V_{milk,tot}$) is divided with 70% ($f_{alveolar}$) (see Table 1) in the alveolar space (the alveolar lumen plus the ducts and the residual, see below) and 30% (1-$f_{alveolar}$) in the cistern (Ayadi *et al*, 2003; Caja *et al*, 2004).

At each milking of the cows, the volume of milk collected ($V_{milk,obs}$) corresponded to 95% (1-$f_{residual}$) of $V_{milk,tot}$ with 5% ($f_{residual}$) remaining in the alveolar space ($V_{residual}$) (Whittem,

2012), regardless of the value of inter-milking interval (IMI). In goats, $f_{residual}$ was considered to be 13% for an IMI of 16h and 19% for an IMI of 8h (Peaker and Blatchford, 1988).

In the current PBPK model, the volume of milk produced over a milking interval (V_{milk} (t)) used to compute the milk concentrations over time, is presumed to increase linearly over time until reaching the $V_{milk,obs}$ at the end of the milking interval (*i.e.,* when t = IMI). In this study, the volume of the available alveolar milk ($V_{alveolar}$ or milk volume of alveolar space and ducts, minus the residual milk) and the volume of the cisternal milk ($V_{cisternal}$) so that $V_{milktot}$, or total milk, was defined as the sum of alveolar, cisternal, and residual milk volumes (*e.g.*, $V_{milktot} = V_{alveolar} + V_{residual} + V_{cisternal}$).

Linear production of V_{milk}, $V_{alveolar,}$ and $V_{cisternal}$ is described in the following equations (Equations 12-14):

$$V_{milk}(t) = (1 - f_{residual}) \times V_{residual} + t \times \left(\frac{V_{milk,obs} - (1 - f_{residual}) \times V_{residual}}{IMI} \right) \quad (12)$$

where $f_{residual}$ is the fraction of residual milk; $V_{residual}$ is the volume of milk remaining in the udder after the previous milking; *t* represents the time since the last milking; $V_{milk,\ obs}$ the volume of milk collected at each milking; and IMI the inter-milking interval (8 or 16h).

Thus,

$$V_{milk,tot}(t) = \frac{V_{milk}(t)}{1 - f_{residual}}$$

Hence,

$$V_{alveolar}(t) = (f_{alveolar} - f_{residual}) \times V_{milk,tot}(t) \quad (13)$$

$$V_{cisternal}(t) = (1 - f_{alveolar}) \times V_{milk,tot}\ (t) \quad (14)$$

2.3.4.2. Drug distribution in udder and in milk

The pH of milk was inferred to be 6.68 for cattle and 6.65 for goats (Park *et al*, 2007) (see Table 1). As described above, OTC in milk is distributed within the fats and aqueous phases and bound to casein, whey, and ionized calcium and magnesium.

Milk concentrations of fat, casein, and whey proteins were calculated based on experimentally measured butyrous and protein rates (**see Table S1 in supplementary materials**). The concentration of fat (g/L) was determined by multiplying the butyrous rate measured (g/kg) by the density of milk (kg/L) (Park *et al*, 2007). The total milk protein concentration (g/L) was determined by multiplying the protein rate measured (g/kg) by the density of the milk. The concentrations of casein and whey proteins were calculated according to their respective proportions in the milk of each species (*i.e.*, 88/12% for cows and 65/35% for goats) (Balthazar *et al*, 2017).

The percentage of free magnesium in milk (16%) was obtained in the literature (Oh and Deeth, 2017) and multiplied by the total concentration of magnesium in milk of each species (Balthazar *et al*, 2017) to obtain the ionized concentration of magnesium (see Table 1). The percentage of free calcium in milk was estimated in cow's milk based on the ratio of free calcium concentration (Neville and Watters, 1983) to total calcium concentration (Balthazar *et al* . Due to missing values for free calcium concentration in other species, this percentage in cattle was multiplied by the total calcium concentration in milk of each species (Balthazar *et al*, 2017) to obtain the ionized calcium concentration (see Table 1).

Affinity constants for fat (ka_{fat}) and casein (ka_{casein}) were estimated from the measurement of milk distribution of 15 drugs, published by Shappell and Lupton (Lupton *et al*, 2018; Shappell *et al*, 2017). The ka_{fat} and ka_{casein} of each drug was calculated as the ratio of the concentration in fat--or the concentration bound to casein--to the free concentration in milk (total concentration in milk multiplied by the free fraction in milk). Then, a linear regression was built between the logarithm of ka_{fat} and the distribution coefficient (logD) of each drug ($R^2 = 0.83$) (Equation 15) and another between the logarithm of ka_{casein} and the distribution coefficient of each drug ($R^2 = 0.80$) (Equation 16). Finally, the ka_{fat} and ka_{casein} of OTC in milk and IW were calculated based on the logD of OTC using these equations.

$$\log(ka_{fat}) = 0.49 \times \log D - 3.112 \quad (15)$$

$$\log(ka_{casein}) = 0.29 \times \log D - 2.09 \quad (16)$$

with $log\ D = \log P - \log X$ for IW

$log\ D = \log P - \log Z$ for milk

462 The affinity constant of OTC for whey proteins (ka_{whey}) was found in the literature
463 (Shappell *et al*, 2017).

464

465 The affinity constants of OTC for calcium ($ka_{Ca^{2+}}$) and magnesium ($ka_{Mg^{2+}}$) were
466 estimated based on the results of Carlotti *et al* (Carlotti *et al*, 2012). Similar to fat and casein,
467 a linear regression was built between the logarithm of the OTC affinity constant for both
468 metal ions (ka_{Ion}^{2+} in L/mol) and the pH ($R^2 = 0.99$) (Equation 17). Thus, the ka_{Mg}^{2+} and
469 ka_{Ca}^{2+} were converted in L/g by dividing ka_{Ion}^{2+} by the molecular weight of each metal ion
470 and calculated as a function of the pH of IW or milk.

471

$$\log(ka_{Ion^{2+}}) = 0.7085 \times \text{pH} - 2.0478 \quad (17)$$

472

473 where ka_{Ion}^{2+} is in L/mol and pH is the pH of IW (7.0) or milk (6.68 for cows, 6.65 for goats).

474 Hence, the unbound fraction in milk was defined in equation 18:

$$fu_{milk} = \frac{1}{\left(1+ka_{fat}\times[fat]+ka_{casein}\times[casein]+ka_{whey,prot}\times[whey,prot]+ka_{Mg^{2+}}\times[Mg^{2+}]+ka_{Ca^{2+}}\times[Ca^{2+}]\right)} \quad (18)$$

475 (**see calculation details in section 2.3.2.3 of the supplementary materials.**)

476 The amount of drug in the alveolar ($A_{alveolar}$) and cisternal ($A_{cisternal}$) milk were described
477 by the following equations (Equations 19- 20):

$$\frac{dA_{alveolar\ milk}}{dt} = CL_{diff,can} \times \left(\frac{Cu_{IW}}{X} - \frac{Cu_{alveolar}}{Z}\right) - Q_{cistern} \times C_{alveolar} \quad (19)$$

$$\frac{dA_{cisternal\ milk}}{dt} = Q_{cistern} \times C_{alveolar} \quad (20)$$

478 with $Q_{cistern} = (1 - f_{alveolar}) \times \frac{V_{milk,obs}}{IMI}$; $Cu_{alveolar} = \frac{A_{alveolar}}{V_{alveolar}} \times fu_{milk}$

479

where $CL_{diff,can}$ is the passive diffusion clearance across the canalicular membrane; X and Z the ionization ratios in IW and alveolar milk; $Q_{cistern}$ the flow of milk from alveoli to cistern; $C_{alveolar}$ the OTC concentration in the alveolar milk; Cu_{IW} and $Cu_{alveolar}$ the OTC free concentrations in IW and alveolar milk; fu_{milk} the unbound fraction of OTC in milk; $f_{alveolar}$ the fraction of alveolar milk; and $V_{alveolar}$ is the volume of alveolar milk.

Finally, the milk concentrations used for the PBPK model predictions over time (Equation 21) were calculated as the sum of alveolar and cisternal amounts of OTC divided by $V_{milk}(t)$, as defined in Equation 12.

$$C_{milk}(t) = \frac{A_{cisternal}(t) + A_{alveolar}(t)}{V_{milk}(t)} \quad (21)$$

Parameters generally used to describe and evaluate the passage of a molecule into milk, such as the milk to plasma ratio (M/P) (Equation 22), the milk clearance (CL_{milk}) (Equation 23), and the percentage of the dose excreted in milk ($Dose_{percentage,milk}$) (Equation 24), were calculated.

$$M/P = \frac{AUC_{0-t,milk}}{AUC_{0-t,plasma}} \quad (22)$$

$$CL_{milk} = \frac{A_{excreted}}{AUC_{96h,plasma}} \quad (23)$$

$$Dose_{percentage,milk} = \frac{A_{excreted}}{Dose \times BW_i} \quad (24)$$

With $AUC_{0\text{-}t}$ the area under the curve of milk or plasma total OTC concentrations over time (t); $A_{excreted}$ the total amount of OTC excreted in milk as predicted by the model; Dose the weight-adjusted dose (10 mg/kg); and BW_i the body weight of animal "i".

Table 1: Parameter values used in the PBPK Model.

Parameters in g/kg in the literature were converted to g/L using udder density (1.06 kg/L) (Upton, 2008) or milk density (1.031 kg/L for cows, 1.034 kg/L for goats) (Park *et al*, 2007). One value per row means that the same value was used for both species. The parameters identified by an asterisk were evaluated in the global sensitivity analysis (see section 2.6).

Parameter		**Abbreviation**	**Cow**	**Goat**
Species physiology				
Alveolar fraction *		$f_{alveoli}$	0.7[1]	
Blood cell pH *		pH_{BC}	7.22[2]	
Plasma pH *		pH_P	7.4[2]	
Udder extracellular water pH *		pH_{EW}	7.4[2]	
Udder intracellular water pH *		pH_{IW}	7.0[2]	
Milk pH *		pH_{milk}	6.68[3]	6.65[3]
Udder vascular fraction*		f_{VASC}	0.12[4]	
Udder extracellular water fraction *		f_{EW}	0.44[5]	
Udder intracellular water fraction *		f_{IW}	0.24[5]	
Udder neutral lipid fraction *		f_{NL}	0.0120[a]	
Udder neutral phospholipid fraction *		f_{NP}	0.0094[a]	
Plasma albumin (g/L) *		alb_P	30.81[6]	31.80[7]
Udder extracellular albumin (g/L) *		alb_{EW}	14.52[8]	
Udder intracellular calcium (g/L) *		Ca^{2+}_{IW}	0.0114[9,10]	
Udder intracellular magnesium (g/L) *		Mg^{2+}_{IW}	0.024[11]	
Milk calcium (g/L) *		Ca^{2+}_{MILK}	0.08[9,10]	0.0931[9,10]
Milk magnesium (g/L) *		Mg^{2+}_{MILK}	0.018[10,12]	0.024[10,12]
Molecule parameters				
Compound type			Zwitterion of group 2[13]	
pKa of acid function *		pKa_{Acid}	7.25[14]	
pKa of basic function *		pKa_{Base}	5.80[14]	
Partition coefficient between octanol and water *		logP	-4.54[14]	
Fraction unbound in plasma *		fu_p	0.81[15]	0.80[b]
Intramuscular bioavailability *		F_{IM}	0.88[16]	0.92[17]
Intramuscular absorption rate (1/h) *		k_{IM}	0.17[c]	0.45[c]
Total plasma clearance (L/h/kg) *		CL_{plasma}	0.09[d]	0.14[e]
Dose fraction excreted unchanged in urine		$fe_{kidneys}$	0.85[18]	
Blood to plasma ratio		BP	0.79[f]	0.82[f]
Partition coefficient	Muscle *	k_{muscle}	0.90[19]	0.89[19]
	Lung *	k_{lung}	2.30[20]	2.27[20]
	Kidneys *	$k_{kidneys}$	6.62[19]	6.54[19]
	Liver *	k_{liver}	1.87[19]	1.84[19]
	Adipose *	k_{fat}	0.09[19]	0.09[19]
	Lumping	k_{rest}	1.41[g]	2.03[g]
Udder permeability				
Capillary radius (mm) *		r	0.0025[21]	
Udder blood flow fraction to lobules *		$fvasc_{Lobules}$	0.98[22]	
PAMPA permeability (cm/s) *		Papp	$1.4 * 10^{-7}$ h	

[a] Calculation based on lipid repartition of Kinsella *et al* (Kinsella and McCarthy, 1968) and total phospholipid concentration of Bruce *et al* (Larson, 1978).

[b] This value is the average of the unbound fraction in cows and sheep from Ziv *et al* (Ziv and Sulman, 1972).

[c] These values were estimated by fitting the PBPK model with experimental plasma data (see section 2.2).

[d] This value is the average between plasmatic clearance of the empirical model of Craigmill *et al* (Craigmill *et al*, 2004) and Nouws *et al* (Nouws *et al*, 1985b).
[e] This value is the average between plasmatic clearance from Aktas *et al* (Aktas and Yarsan, 2017) and Rule *et al* (Rule *et al*, 2001).
[f] **See calculation details in Supplementary Material.**
[g] See equation 4 in the text.
[h] Experimental data (see section 2.1.2).
Sources: [1](Ayadi *et al*, 2003; Caja *et al*, 2004); [2](Rodgers *et al*., 2005); [3](Park *et al*., 2007); [4](Snipes and Lengemann, 1972); [5](Konar *et al*, 1972); [6](Bobbo *et al*, 2017); [7](Alberghina *et al*., 2010); [8](Vestweber and Al-Ani, 1984); [9](Neville and Watters, 1983); [10](Balthazar *et al*, 2017); [11](Martens and Stumpff, 2019); [12](Oh and Deeth, 2017); [13](Rodgers and Rowland, 2006); [14]("Chemicalize - Instant Cheminformatics Solutions," n.d.); [15](Ziv and Sulman, 1972); [16](Nouws *et al*, 1985a); [17](Rule *et al*., 2001); [18](Nouws *et al*, 1985b); [19](Craigmill, 2003); [20] (Achenbach, 1995); [21](Prosser, 1996); [22](Thompson, 1980).

2.4. Model calibration

Individual plasma concentrations measured in the current study (study A, see Table 2) were used to calibrate the rate of OTC absorption after IM administration (k_{IM}). The PBPK model with all parameters fixed (except k_{IM}) was used (see Table 1) and only k_{IM} and its standard deviation were estimated using the Stochastic Approximation Expectation-Maximization (SAEM) algorithm method, for each species. For cows, four (4) concentrations in milk and 8 concentrations in plasma were reported as below the LOQ. For goats, sixteen (16) concentrations in milk and nineteen (19) concentrations in plasma were reported as below the LLOQ. Data below the LOQ were treated as left-censored observations using the M4 method (*i.e.*, the likelihood that they were between zero (0) and the LLOQ) was calculated) (Beal, 2001).

The residual errors (RV) of the PBPK model were set to the value of the intermediate precision of the analytical method (see section 2.1.4) in plasma and milk for each species, assuming that the errors due to model misspecification or other unknown sources were negligible.

Table 2: Experimental studies of OTC in cows and goats used for calibration and validation of the PBPK Model

Modelling purpose	Study ID	Route	Dose (mg/kg)	Species (n)	BW (kg)	Matrix	IMI	V_{milk}	TB, TP
Calibration (estimation of k_{IM})[1]	A	IM	10 (SD)	Cow (6), Goat (6)	568	P	8h, 16h	Yes[a]	Yes[b]
Internal evaluation[1]	A	IM	10 (SD)	Cow (6), Goat (6)	568	M	8h, 16h	Yes[a]	Yes[b]
External evaluation[2]	B	IV	5 (SD)	Cow (19)	603	P, M	NA	NA	NA
External evaluation[3]	C	IM	10 (5 doses, OD)	Cow (20)	577	M	12h	Yes[a]	NA
External evaluation[3]	D	IV	10 (SD)	Cow (4)	643	M	12h	Yes[a]	NA
External evaluation[3]	E	IV + IM	10 (SD) for IV + 10 (4 days,OD) for IM	Cow (4)	634	M	12h	Yes[a]	NA
External evaluation[4]	F	IM	20 (SD)	Goat (5)	56	P, M	24h	NA	NA
External evaluation[4]	G	IV	20 (SD)	Goat (5)	56	P, M	24h	NA	NA

[a] At each milking; [b] Once per animal before OTC administration
Note: IM: intramuscular; k_{IM}: intramuscular absorption rate; IV: Intravenous; SD: single dose; OD: once daily; P: plasma; M: milk; NA: not available; IMI: inter-milking interval; V_{milk}: Volume of milk measured, TB: butyrous rate; TP: protein rate.Sources: [1]Current study; [2](Nouws *et al*, 1985a); [3]Unpublished study; [4](Rule et al., 2001)

2.5. Establishment of the Population PBPK (popPBPK) Model

Monte Carlo simulations were performed to generate a virtual population of cows and goats (n=1000 each) taking into account the inter-individual variability (IIV) and uncertainties of the parameters from the PBPK model. A log-normal distribution was assumed for all parameters because of their asymmetric distribution and their strictly positive values (Fenneteau *et al*, 2009), and was assumed to represent the IIV (for physiological parameters)

556 and uncertainty (for physico-chemical parameters). Coefficients of variation (CV) were
557 found in the literature based on previous experimental data or set at 30% for physiological and
558 20% for drug-related parameters with no experimental values, (**see Table S3 for cow and S4**
559 **for goat in the section 2.4 of the supplementary materials**) (Clewell and Clewell, 2008;
560 Henri *et al*, 2017a; Li *et al*, 2019a).

561

562 The code was written to ensure that the sum of the volume fractions or that of the blood
563 flow fractions did not exceed 1, (Fisher *et al*, 2020) (**see code in section 4. of the**
564 **supplementary materials**).

565

566 2.6. Model Evaluation: Validation and Sensitivity Analysis

567 The evaluation of the popPBPK model was carried out by graphical goodness-of-fit
568 (GOF) and statistical criteria, with an internal validation comparing the model predictions to
569 the experimental data generated in the study (study A), and an external validation comparing
570 the predictions to data from the literature and unpublished data (studies B to G, see Table 2).
571 If predictions fell within a factor of 2 of the experimental data, the popPBPK model was
572 considered as acceptable by the World Health Organization (WHO) (WHO *et al*, 2010). The
573 mean absolute percentage error (MAPE) and the determination coefficient (R^2), based on
574 linear regression of model observations *vs* simulations, were also calculated to assess GOF
575 and model performance (Cheng *et al*, 2016). The popPBPK model was considered as valid if
576 the MAPE value was lower than 50% and the R^2 was at least 0.75 (Li *et al*, 2018) (Li *et al*,
577 2019b). Visual Predictive Checks (VPC) were generated by performing Monte Carlo
578 simulations (n= 1000 animals), considering both IIV and RV. The milk and plasma
579 predictions interval (PI) (5^{th} and 95^{th} percentiles) were plotted against the experimental data.

580

581 The external validation was conducted using average concentrations (and the standard
582 deviation if available) from external and independent datasets for each species treated with a
583 conventional OTC formulation with different dosing regimens (dose and route of
584 administration) (studies B to G see Table 2). Plasma and milk data found in the literature
585 were extracted from selected studies using WebPlotDigitizer (version 4.4, year 2020,
586 California USA, https://automeris.io/WebPlotDigitizer).

For study B, the IMI was not specified in the article and was set at eight (8) and sixteen (16) hours, as in the current study. When some parameters were not specified, such as volume of milk produced per milking (for studies B, F and G), and fat, casein, and protein levels (for all external data sets), they were simulated (as explained below).

In order to simulate milk volumes of the 1000 animals, a linear mixed effects model (SAEM algorithm with Monolix software) was fit to to the experimentally measured milk volumes (study A, see Table 2) (performed separately for cows than for goats). This model included an intercept, an effect of milking interval, and inter- and intra- animal variability. From this model different volumes of milk for each animal (n=1000) at each milking could be simulated.

To simulate the milk fat, casein and whey proteins levels and the body weights of the 1000 animals, data (mean and dispersion value) was used from the literature ((Balthazar *et al*, 2017; Leitner *et al*, 2004) for milk composition; (Nouws *et al*, 1985a; Rule *et al*, 2001) and unpublished study for body weight) to draw different values for each simulated animal (n=1000) of each species. The nominal doses administered (in mg) were adjusted to match the simulated weights for each animal of each species.

The ability of the model to predict concentrations of OTC in the milk of cows and goats, with other doses and routes of administration, was assessed by comparing the external dataset with the 90% PI from the VPC.

A global sensitivity analysis (GSA), using the "*extended-FAST*" method (Saltelli and Bolado, 1998), was performed to assess the influence of sixty-six (66) input parameters on milk model predictions (**see parameters with an asterisk in Table 1 and Table S2 in supplementary materials**). A uniform law was considered and each parameter was changed by $\pm$10% of the median value, simultaneously (Peters, 2012). With the GSA, input parameter influence could be divided into main effects and total effects where the difference between main and total effects (additional effects) represented parameter interactions. Because total effects are the most robust indicators of PBPK parameter influences (Jarrett *et al*, 2016), they are the only ones discussed here. The outputs considered were the area under the curve of

OTC total concentration in milk between time 0 hours and 96 hours (AUC_{96h}) and OTC total concentration in milk at 96 hours (C_{96h}). Total effects above the typical threshold value of 0.1 indicated significantly sensitive parameters (Jarrett *et al*, 2016; Li *et al*, 2017; Peters, 2012).

Moreover, variations of a factor 10 of the nominal value of the Papp, which can vary far more than 10% between drugs, have been explored (see section 3.3).

2.7. Model Application

An estimation of the withdrawal period (WP) in milk was performed using the popPBPK model, based on results of the Monte Carlo simulations (n=1000) with the IIV but without the RV, with the standard dosing regimen specified in the SPC of the Terramycin® speciality (*i.e.*, 10 mg/kg/day for four (4) days or 5 mg/kg/day for three (3) days by IM route). The time (rounded up to the next whole day) for which the 99th percentile is equal to the MRL (100 µg/kg for milk) since the last injection was defined as the (predicted) WP in milk. Volume of milk and rate of milk fat, casein, and whey proteins, of each animal were drawn as explained above (see section 2.6). Body weights were simulated based on mean and dispersion values from the literature (Lautz *et al*, 2020).

2.8. Software

Monolix (version 2020R1. Antony, France: Lixoft SAS, 2020) was used to develop the popPBPK model and Simulx (version 2020R1. Antony, France: Lixoft SAS, 2020) to run all simulations. (**See the model code available in Supplementary Materials**). Graphs were generated using GraphPad Prism (version 9.1.0 for Windows, GraphPad Software, San Diego, California USA, www.graphpad.com). GSA was performed with Rstudio (v 1.4.1106, RStudio Team, 2009-2021, PBC, Boston, MA, http://www.rstudio.com/) and the sensitivity package (v 1.26.0; Iooss 2021; https://CRAN.R-project.org/package=sensitivity).

3. **Results**

3.1. Model Calibration

The observed plasma data BLQ (18%) were used to estimate only the IM absorption rates (k_{IM}) for each species with a very good confidence (RSE < 15%), given a typical value of 0.17 1/h and 0.45 1/h for cows and goats, respectively (**see section 3.1.1 of the supplementary materials**). The associated IIV values (used for the popPBPK model application, see below) were equal to 22% for cows and 30% for goats, with rather good precision (RSE < 30%).

3.2. Simulations from the popPBPK Model

One thousand (1000) virtual individuals of each species with specific body weight, volume, and composition of milk produced were simulated (**see the distribution and range of all parameters of these virtual populations are presented in section 2.4. of the supplementary materials**).

3.3. Model Evaluation: Validation and Sensitivity Analysis

For internal validation using the observed concentrations from the current study (study A, see Table 2), the VPC showed that most of the observed data (95%) in both plasma and milk were within the 90% PI for both species (Figure 2 for cows and Figure 3 for goats). The BLQ data were also well predicted.

In cow's milk (Figure 2B and D), 73% of typical predictions were within a factor of 2 of the experimental data. The R^2 and the MAPE were 0.92 and 29%, respectively, which met the validation criteria in cow's milk (Figure 2F).

Similarly, to the cow model, 67% of the typical predictions in goat's milk were within 2-fold of the experimental data (Figure 3B and D). The R^2 and MAPE of 0.99 and 12%, met the validation criteria in goat's milk (Figure 3F). The internal validation of our popPBPK model, based on this experimental data, was therefore considered successful.

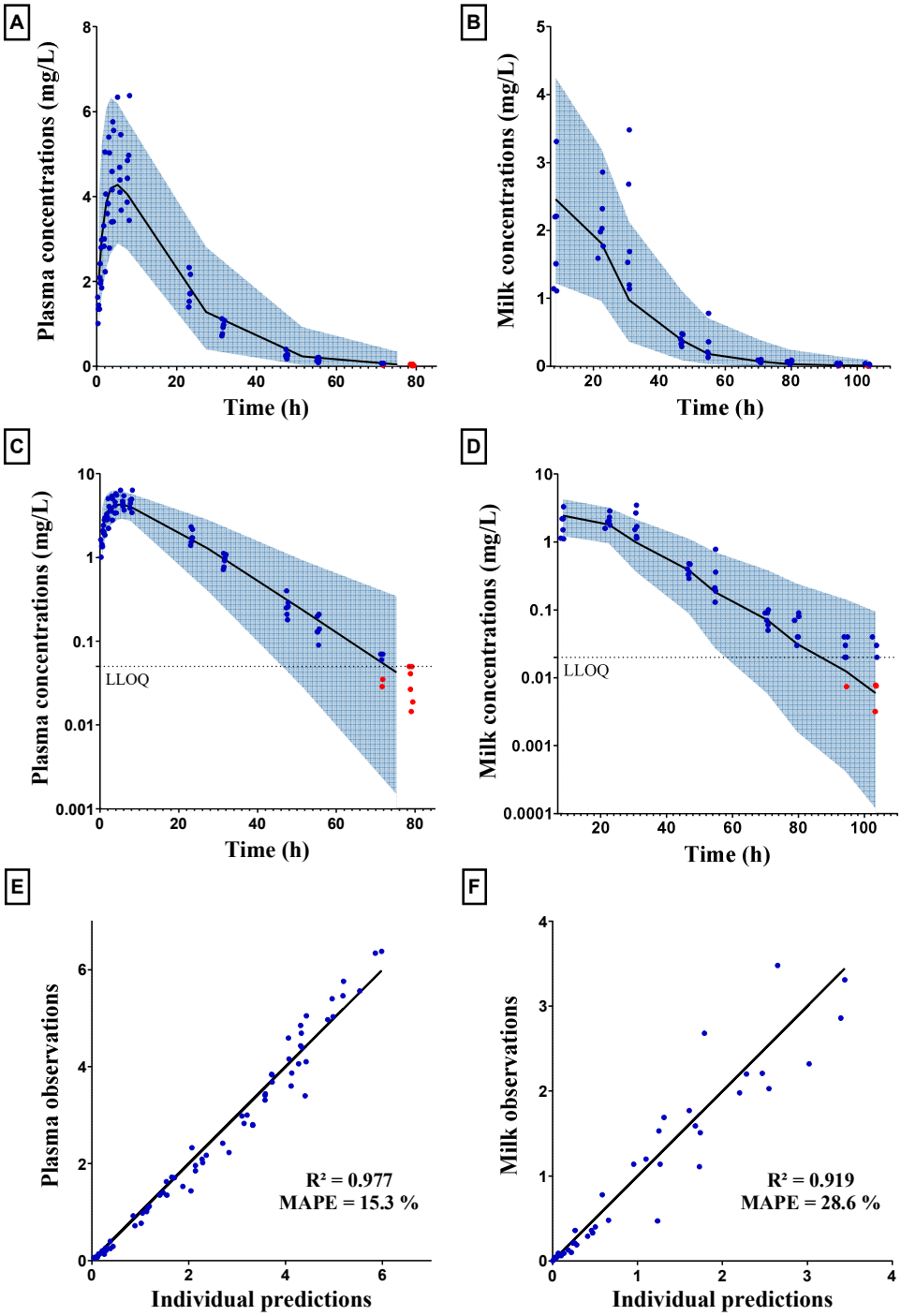

Figure 2: Visual predictive check of OTC concentrations in cow plasma (A, C) and milk (B, D) using the popPBPK model. The median is represented by a solid black line and the 90% prediction interval is represented by the area in blue. The experimental data (individual data points) from the current study are represented with circular points. The dotted line represents the lower limit of quantification (LLOQ, 0.05 µg/ml for plasma, 0.02 µg/ml for milk). Data below the LLOQ are marked in red and estimated by the model. The bottom graphs illustrate the result of a regression analysis between model predictions and measured OTC concentrations in plasma (E) and in milk (F). The coefficient of determination (R^2) and mean absolute percentage error (MAPE) are shown in the graphs.

677

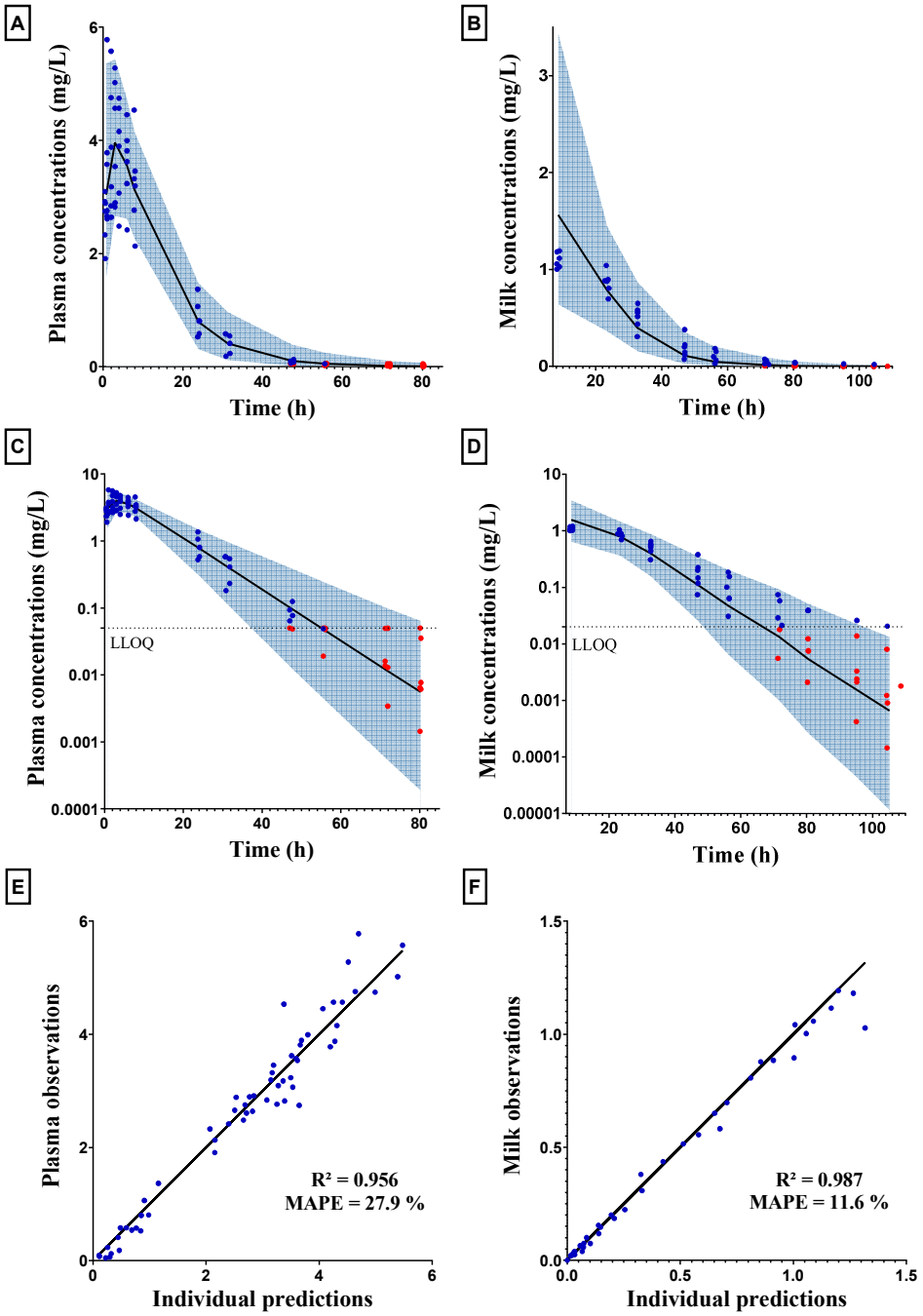

Figure 3: Visual predictive check of OTC concentrations in goat plasma (A, C) and milk (B, D) using the popPBPK model. The median is represented by a solid black line and the 90% prediction interval is represented by the area in blue. The experimental data from the current study are represented by circlular points. The dotted line represents the lower limit of quantification (LLOQ, 0.05 µg/ml for plasma, 0.02 µg/ml for milk). Data below the LLOQ are marked in red and estimated by the model. The bottom graphs represent the result of a regression analysis between model predictions and measured OTC concentrations in plasma (E) and in milk (F). The coefficient of determination (R^2) and mean absolute percentage error (MAPE) are shown in the panel.

For the external validation in cows, **(see Figures S3 and S4 of the supplementary materials)**, after IV of 5 mg/kg (study B, see Table 2), the model underestimated the initial plasma concentration (the typical predictions for the first 0.6 hours were 33-47% of the

observed mean values), but concentrations measured at late time points were well predicted (within a factor of 2 after one-hour post administration). In milk, 86% of the predictions were within a factor of 2 of the observed data. After five (5) IM administrations of 10 mg/kg/day (study C), the model well predicted (within a factor of 2) milk concentrations up to 168 hour and under-estimated the final time points (predictions of the final time points were lower than 37% of the observed data). Overall, 78% of the milk predictions were within a factor of 2 of the observed data. After IV administration of 10 mg/kg (study D), the model underestimated the initial plasma concentrations, predicted milk concentrations well for up to ninety-six (96) hours post-administration, but under-estimated the final time points. The LLOQ of the unpublished data was 0.01 µg/mL, and 3, 4, 2, and 4 animals were BLQ at 108 hours, 120 hours, 132 hours, and 144 hours after administration, respectively. After one IV and four IM injections of 10 mg/kg (study E), 72% of the predictions were within a factor of 2 of the observed data.

For the external validation in goats, (**see Figure S5 A-B in the section 3.2 of the supplementary materials**), after IM administration of 20 mg/kg (study F), the model slightly underestimated the final time points in plasma (but still within a factor of 2). In milk, 60% of model predictions were within a factor of 2 of the observed data. After IV administration of 20 mg/kg (**see Figure S5 C-D in the section 3.2 of the supplementary materials**) (study G), the model overpredicted the late plasma concentrations. In milk, 88% of predictions were within a factor of 2 of the observed data.

Overall, based on external data on OTC concentrations in cow or goat milk from the literature or unpublished dataset, the popPBPK model was considered to be valid.

A GSA was carried out for sixty-six (66) parameters of the PBPK model, (**identified by an asterisk in Table 1 and Table S2 in supplementary materials).** The results are presented in Figure 4 for AUC_{96h} and C_{96h} in cow and goat milk. Three parameters having a sensitivity coefficient (total effect) higher than 0.1 were considered to have a significant impact on AUC_{96h} for both species. Seven (7) parameters for cows and height parameters for goats were considered to have a significant impact on C_{96h}.

715 The predicted AUC_{96h} in milk was sensitive to the acid pKa of OTC (0.42 for cows, 0.48
716 for goats), the pH of EW (0.39 for cows, 0.42 for goats) and the pH of milk (total effect of
717 0.15 for both species). The predicted C_{96h} in milk was also sensitive to these three parameters
718 but also to the pH of IW (0.77 for cows, 0.80 for goats), the total plasma clearance (CL_{plasma},
719 coefficient of 0.23 for cows, 0.34 for goats), the partition coefficient in muscle (k_{muscle},
720 coefficient of 0.21 for cows, 0.56 for goats), and in kidneys (k_{kidney}, coefficient 0.10 for cows
721 and of 0.54 for goats), and to the F_{IM} (0.13) for goats.

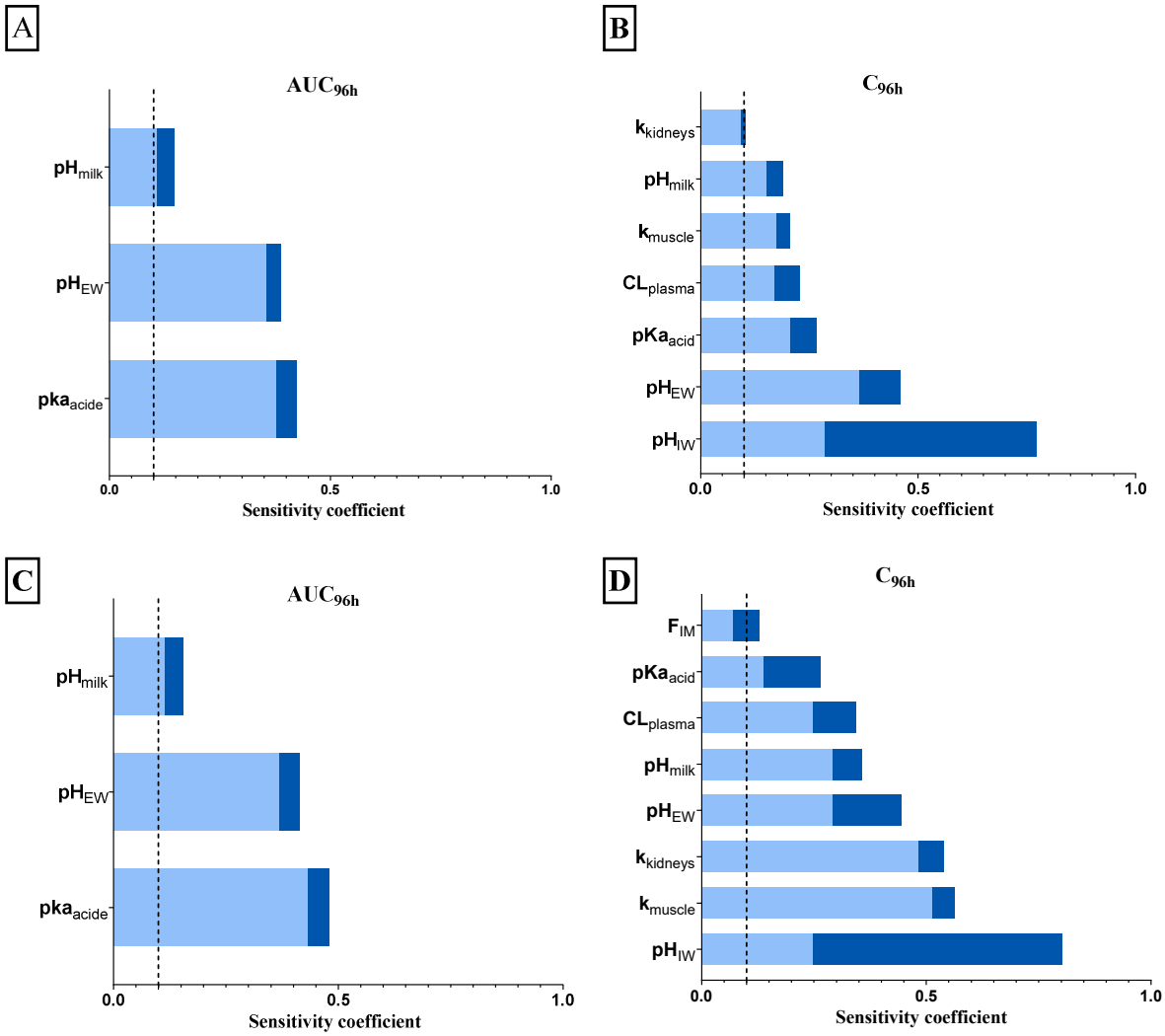

Figure 4: Global sensitivity analysis of the PBPK model of OTC in cow milk (upper panel) and in goat milk (lower panel). The sensitivity coefficient was estimated after a + 10% variation of the sixty-six (66) input parameters on OTC area under the curve (AUC) between 0 and 96h (A, C), and concentration at 96h in milk (B, D). The main effects are presented in light blue and total effects in dark blue. The dotted lines represent the threshold of 0.1 for determining the impact of a parameter.

722

723 To illustrate the influence of the milk pH, a change of 10% of its initial value in cows
724 (6.68), resulted in a variation of the AUC of its initial value (68 mg/L.h) ranging from -18%

725 (56 mg/L.h) when the pH is lower (6.01) to +84% (125 mg/L.h) when the pH is higher (7.35)
726 (see Figure 5A).

727

728 To illustrate the influence of the OTC acid pKa, a 10% change in its initial value (7.25),
729 resulted in a variation of the AUC of its initial value (68 mg/L.h) ranging from -60% (28
730 mg/L.h) when the acid pKa is lower (6.53) to +67% (113 mg/L.h) when the pH is higher
731 (7.98) (see Figure 5B).

732

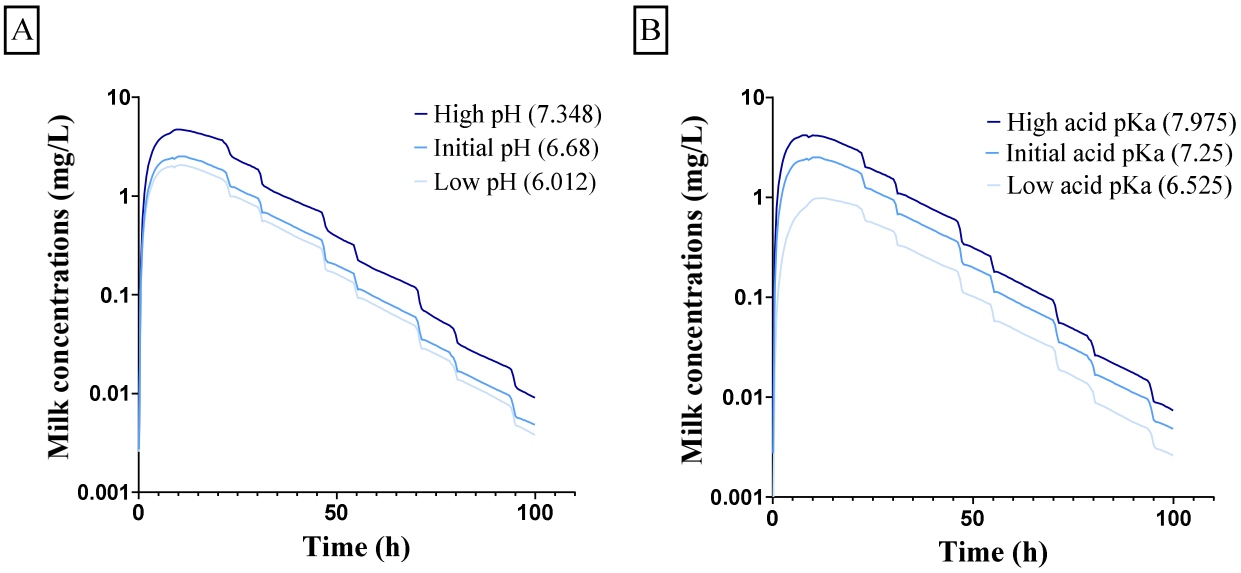

Figure 5: PBPK model predictions of OTC in cow milk with a variation of ± 10% of milk pH (A) and acid pka of OTC (B).

733

734 The impact of permeability (Papp) on OTC excretion into milk with hypothetical lower or
735 higher permeability was also evaluated. The concentration profiles in cow's milk are
736 presented for four (4) different Papp values in Figure 6. Thus, when Papp increases from 1.4
737 x 10^{-8} cm/s (molecules with very low permeability) to 1.4 x 10^{-5} cm/s (molecules with high
738 permeability), the model predicts that AUC_{96h} increases by 626% (from 17 h.mg/L to 103
739 h.mg/L). Furthermore, in this case T_{max} in milk decreases from 19 hours to 6 hours and the
740 maximum concentration (C_{max}) increases from 0.4 mg/L to 4 mg/L. However, between a
741 Papp of 10^{-5} (AUC_{96h} of 103 h.mg/L) and 10^{-6} cm/s (AUC of 99 h.mg/L), the impact on AUC
742 was negligible.

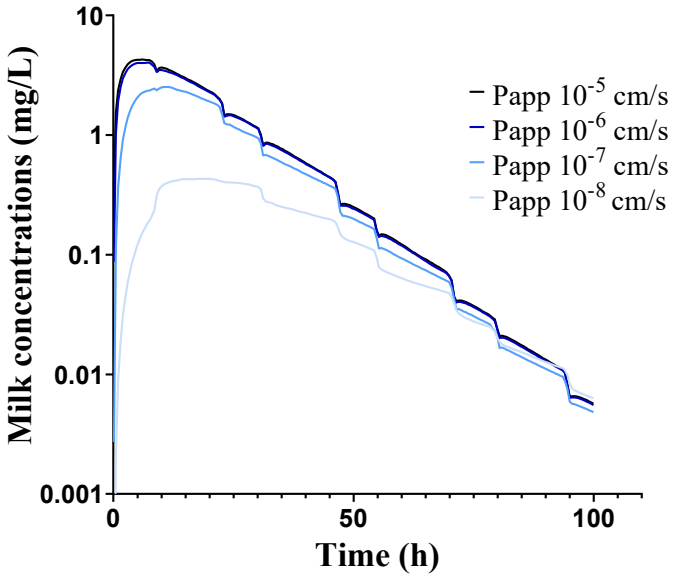

Figure 6: PBPK model predictions of OTC in cow milk with a variation of Papp from 10^{-8} to 10^{-5} cm/s.

743

744 3.4. Drug distribution in udder and milk

745 The total and free OTC concentrations, over time, within the plasma, udder sub-
746 compartments, and the milk as predicted by the popPBPK model are presented in
747 supplementary materials in Figure S6 A, C for cows and Figure S7 A, C for goats. Free
748 concentrations were higher in plasma and EW (which were superimposed) than in IW and
749 milk. In comparison, total concentrations were higher in IW but still lower than those in
750 plasma and EW. The elimination slopes were parallel in all sub-compartments. In total
751 concentrations, the T_{max} in plasma and EW were equivalent (5 hours for cows, 3 hours for
752 goats), whereas that of IW (7.5 hours for cows, 6 hours for goats) and milk (11 hours for
753 cows, 8 hours for goats) were delayed.

754

755 Proportions of free or bound OTC to each component are detailed on Figure S6 B for
756 cows and Figure S7 B for goats in supplementary materials. In plasma and EW, the model
757 predicts that OTC is mainly in unbound form (about 81% and 90% respectively) and weakly
758 bound to albumin. In IW, the model predicts that OTC is more strongly bound (the unbound
759 fraction is about 47%) and that binding is mainly to magnesium (Mg^{2+}). In milk the model
760 predicts that OTC is approximately 60% bound: primarily to Ca2+ (~40%) and Mg2+
761 (~15%).

762

763 Proportions of ionized or unionized OTC in each sub-compartment are presented in
764 Figures S6 D for cows and S7 D for goats in supplementary materials. The fraction of ionized
765 OTC was predicted to be 60% in plasma and EW (pH=7.4), 39% in IW (pH=7.0), and 29% in
766 milk (pH=6.68 for cows, 6.65 for goats), highlighting again the strong influence of pH on
767 OTC distribution.

768

769 Based on the results of the popPBPK model, the ratio of M/P (Eq 22, calculated
770 between 0 hours and 96 hours), was 0.7 for cows and 0.5 for goats. The CL_{milk} was estimated
771 as 0.44 L/h (7.76 $*10^{-4}$ L/h/kg) and 0.051 L/h (7.67 $*10^{-4}$ L/h/kg) for cows and goats,
772 respectively.

773

774 Overall, 0.75% of the dose was excreted in the milk for cows, whereas it was 0.50 % for
775 goats.

776

777 3.5. Model Application

778 In milk, the WP after IM injections of 10 mg/kg/day for four (4) days and 5 mg/kg/day
779 for three (3) days were, predicted to be five (5) and four (4) days respectively for cow milk,
780 whereas it was predicted to be four (4) and three (3) days for goat milk (Figure 7).

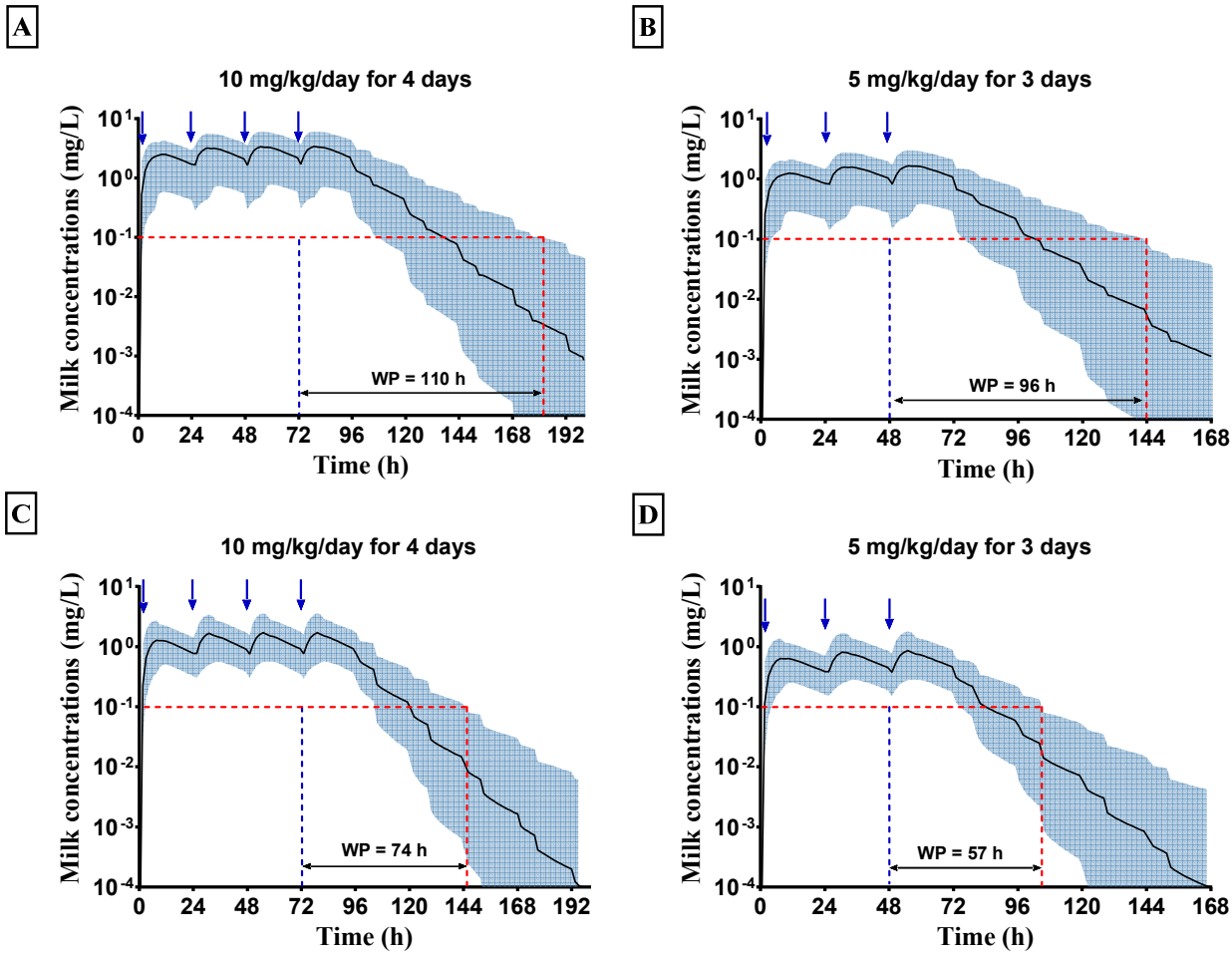

Figure 7: Simulation of OTC administration in 10 mg/kg/day for four (4) days (A,C) and 5 mg/kg/day for three (3) days (B,D) by IM route in cow (A,B) and goat milk (C,D). The maximum residue limit (MRL) is represented by red dotted horizontal lines and the time when the 99th percentile is equal to the MRL by red dotted vertical lines. WP is calculated by the difference between this time and the time of the last injection: seventy-two (72) hours or forty-eight (48) hours.

781

782

783 **4. Discussion**

784 4.1. PBPK model objectives

785 A generic popPBPK model was developed, detailed in terms of udder physiology and
786 milk composition, in order to exploit it to various compounds and species. To illustrate its
787 usefulness, the model was used to predict the kinetic of OTC in cow and goat milk.

788

789 This model predicted the OTC concentrations measured in plasma and milk from cows
790 and goats well. In this study, the M/P ratio for the cows was 0.7, which is slightly lower than
791 the previously published value (1.2 to 2), but consistent with the observed value (0.7
792 calculated with a non-compartmental analysis from the observed data) (Nouws *et al*, 1985a).
793 For goats, it was 0.5 (no value in the literature for comparison was found). The predicted

794 percentage of the dose excreted in milk (0.8% for cows and 0.5 % for goats) was equal to that
795 observed with the experimental data.
796
797 The model predictions compared to external data obtained in cows with different
798 dosing regimens were also satisfactory. However, the predicted milk concentrations for more
799 than ninety-six (96) hours after the last administration occasionally underestimated the
800 average concentrations measured (of that found in unpublished studies C, D, E). As these
801 concentrations were well below the quantification limits, this potential bias is perhaps
802 analytical. On the other hand, since the measured plasma concentrations are not available
803 with these external data sets, it cannot known whether this bias is due to poor plasma
804 predictions or only to poor milk predictions. During the external validation, an
805 underestimation of the initial plasma concentrations by this study model was also observed.
806 This bias may be due to choosing to use a flow limited model for the systemic portion. This
807 choice may have been valid for IM administration, but may not be valid for IV administration.
808 Indeed, during an IM administration, the initial distribution phase may be masked by the
809 absorption phase. It would therefore be useful, in order to develop a generic PBPK model, to
810 take into account a model with limited permeability for the systemic portion. This would
811 allow better extrapolation between different types of administration or formulations. Note
812 that if this PBPK model is selected for another formulation than the one used for this study
813 data on the release of the active ingredient as well as the absorption rate from the injection site
814 is available. Either these data are available in the literature, or they have to be determined
815 experimentally, as has been done here.
816
817 In goats, the model correctly predicted external concentrations of OTC in milk after IV
818 and IM of 20 mg/kg (Rule *et al*, 2001), with a slight overestimation of late concentrations
819 after IV administration, because of poor predictions of plasma concentrations.
820
821 4.2. Comparison to other PBPK model
822 4.2.1. PBPK model of OTC in non-lactating species
823 A few PBPK models are available for OTC in non-lactating species. The model of OTC
824 in sheep (Craigmill, 2003) and that of cattle (Achenbach, 1995) allowed the tissue partition
825 coefficients to be obtained for the current PBPK model. The model of Lin *et al* of OTC in
826 dogs (Lin *et al*, 2015) considered some tissues as permeability limited (*i.e.*, fat, muscle, and

slowly perfused tissues), whereas the models of Craigmill and of Riad (Riad *et al*, 2021) considered all tissues as perfusion limited. For the current model, a perfusion-limited model structure was also chosen for tissue distribution, except in the udder, because it adequately predicted the OTC plasma concentrations while avoiding the addition of uncertainties of limited permeability parameters.

Some existing models use a two-compartments model (with two different rates) to describe the IM absorption of a long-acting formulation of OTC (Achenbach, 1995; Lin *et al*, 2015; Riad *et al*, 2021). In the current model, a simple first order absorption was sufficient to correctly predict the plasma kinetic of the conventional formulation of OTC. As the IM absorption rate (k_{IM}) was not available for the target formulation and species, it was estimated with the current plasma data. This was the only parameter that was estimated in the model, with good confidence.

4.2.2. PBPK model of the udder

This new model is the first PBPK model to use a permeability-limited sub-model for the udder, distinguishing the VASC, EW, and IW spaces of the udder. Compared to perfusion-limited models, it allows describing the mechanisms by which slowly equilibrated drugs are distributed into the udder and reach the milk.

The udder IW acted as a deep compartment (see discussion below) in a more physiological manner than the empirical retention compartment mimicking the hypothetical drug adsorption on the alveolar epithelium described by Woodward *et al* (Woodward and Whittem, 2019). Moreover, the low permeability (Papp) of OTC impacted the rate of release into milk.

In the current model, exchanges between milk (alveolar space) and the IW of the udder were considered, mimicking reabsorption into the systemic circulation (Ziv and Sulman, 1975), as discussed by Li *et al* (Li *et al*, 2018).

Similarly to the model by Woodward *et al* (Woodward and Whittem, 2019), the current model considered milk production in the alveoli, transport via the ducts, storage in the cistern, and residual volume remaining in the ducts after milking. This studies model,

however, did not take into account a delay before filling the cistern, but considered a passage of milk from the alveolar space to the cistern at a rate equal to the average rate of increase of the milk volume in the cistern during the milking intervals.

In order to be able to predict milk concentrations over time, and not only at the time of milking, it was assumed a linear increase in the volume of milk produced during the milking intervals. The Hill equation, described in several papers (Li *et al*, 2018; Whittem, 2012; Woodward and Whittem, 2019), mimicking the nonlinear increase in milk volume, was not used because it would have required the estimation of parameters from the volumes of milk measured and it was preferred to use these experimental values directly. Furthermore, the experimental data obtained here showed that milking volume was almost proportional to IMI, which justified the linear increase in volume.

4.3. Factors influencing passage into the milk

In this model the many physiological and physico-chemical factors were taken into account, such as binding to milk components or passive diffusion, that can influence the passage into milk. In the case of the passage of OTC into cow and goat milk, the global sensitivity analysis (GSA) showed that the most influential factors were the ionization (pH and pKa) on AUC_{96h} and the systemic exposure (CL_{plasma} and k_{tissue}) on C_{96h}. The rest of the sixty-six (66) parameters tested in the sensitivity analysis (**see parameters with an asterisk in Table 1 and Table S2 in supplementary materials**) had less impact on the predictions of AUC_{96h} and C_{96h} of OTC in milk.

In addition to the factors identified by the GSA, influence of two other factors is discussed: binding in the whole udder (ka_{Ca}^{2+}, ka_{Mg}^{2+}…) (see section 4.3.3) and OTC permeability (Papp) (see 4.3.4) on the passage of OTC in milk.

888 4.3.1. Systemic circulation

889 In the current model, the exchange between plasma, IW, and milk acts by passive
890 diffusion of the unbound and unionized form of OTC. Therefore, the same AUC_{96h} of the
891 unbound and unionized form of OTC in these 3 compartments, highlighting the strong impact
892 of plasma PK on the passage into milk, was observed. In such a PBPK models, it is therefore
893 important to have a reliable model for the systemic PK to adequately describe the passage of a
894 compound over the blood-milk barrier. That's why the estimation of k_{IM} from was chosen for
895 this experimental animal study.
896
897 A whole PBPK model, including systemic PK was chosen because of the available PK
898 models in cows and goats (*i.e.,* known CL_{plasma}, $fe_{kidneys}$, F_{IM}, and fu_p) and the available PBPK
899 models, allowed the partition coefficients for each tissue to be obtained. In addition, having a
900 complete PBPK model, which is more generalizable, will allow easier future cross-species
901 and cross-molecule extrapolations. Alternatively, a classical compartmental model of the
902 plasma data could have been developed in order to have a reliable plasma PK model, and
903 established a minimal PBPK model including only the udder part as Woodward *et al*
904 (Woodward and Whittem, 2019). This could be interesting for species where physiological
905 data are lacking.
906
907 Plasma clearance had a significant impact on the C_{96h} of OTC in milk. The impact of
908 CL_{plasma} on the terminal elimination slope in plasma and milk explains its influence on the
909 predicted residual concentrations in milk. In this study model, CL_{plasma} was obtained from the
910 literature and split between renal and hepatic clearances based on published data of
911 unchanged excreted fraction in urine (Nouws *et al*, 1985b). This elimination model is not the
912 most mechanistic one and for future cross-species extrapolations, it will have to be adapted
913 with more physiological data of hepatic or renal elimination (*e.g.* glomerular filtration and
914 tubular secretion), using also more mechanistic PBPK model for such pathway (Mevius *et al*,
915 1986; Viel, 2018).
916
917 Among the partition coefficients, the k_{muscle} and the $k_{kidneys}$ significantly affected C_{96h} in
918 the GSA (see Figure 4). As these parameters were used in the calculation of the lumping
919 compartment partition coefficient (k_{rest}, see Equation 4), and since the lumping compartment
920 was the largest compartment in terms of volume (about 40% of the total weight), it is not

921 surprising that these partition coefficients were the most influential on systemic PK,
922 especially on the terminal slope, and therefore milk exposure. As observed in GSA, the
923 impact of $k_{kidneys}$ is greater for goats than for cows. This is probably due to the fact that the
924 volume of the richly perfused tissue is greater in goats (8% of BW *vs* 4% for cows).
925
926 Several methods can be used to predict the k_{tissue} if *in vivo* data are missing from the
927 literature. For comparison, cow k_{tissue} were calculated using the equations of Rodgers and
928 Rowland (RR) (Rodgers *et al*, 2005) (**see Table S6 in section 3.3 of the supplementary**
929 **materials**). Only the k_{tissue} of fat calculated by RR is equivalent to that found in the literature,
930 while the others were lower (by 15% for kidneys to 52% for liver). The much lower systemic
931 distribution predicted using RR k_{tissue} led to much lower plasma and milk elimination half-
932 lives (4.5h *vs* 9.1h in milk and 4.2h *vs* 7.9h in plasma) (**see Figure S8 in the section 3.3 of**
933 **the supplementary materials**). The k_{tissue} obtained from literature allowed a better
934 description of the experimental data, even if the predictions of RR were quite good,
935 confirming that when possible, experimental data should be preferred to predictions from
936 theoretical equations (Yau *et al*, 2020).
937
938 4.3.2. Ionization
939 The current PBPK model accounts for the ionization of OTC in each udder and milk
940 sub-compartments. As observed in GSA, the acid pKa of OTC, as well as the pH of the udder
941 and milk sub-compartments, had a significant impact on the AUC_{96h} and C_{96h} of OTC (see
942 Figure 4).
943
944 Only the unionized form can passively diffuse across physiological membranes, but
945 equilibria are re-established once the membranes are passed depending on the pH of the
946 medium. As the acid pKa of OTC (7.25) is close to the plasma (7.4), IW (7.0) and milk (6.7)
947 pH values, small variations in pKa or pH led to large variations in ionized fractions. Thus,
948 due to the lower pH in milk than in plasma, the ionized fraction was lower in milk (29%
949 instead of 60%). Since the non-ionized concentration of OTC is the same in the different
950 compartments (notably plasma and milk), and the ionized concentration is lower in milk than
951 in plasma, the whole free concentration in milk is predicted to be lower than that in plasma
952 (**see Figure S6 and S7 in supplementary materials**).
953

954 The pKa values of OTC were based on an empirical calculation (Szegezdi and
955 Csizmadia, 2007, 2004) and were comparable to values reported in the literature (Carlotti *et*
956 *al*, 2012; Stephens *et al*, 1956; Tongaree *et al*, 1999). However, as evidenced by these
957 publications, for zwitterions (with multiple chemical groups), it is difficult to determine with
958 certainty to which groups these pKa are assigned. This difficulty is probably related to the
959 determination method and conditions (temperature, solvent) used (Reijenga *et al*, 2013).
960
961 Regarding cells and tissues, due to missing values in the literature for ruminants, pH
962 values were taken from other species (Rodgers *et al*, 2005; Waddell and Bates, 1969). These
963 have been shown to be equivalent for animal cells and tissues from different species (for
964 healthy and un-anesthetized animals). Regarding the milk, the pH is also similar between
965 species. However, it can change over time, *e.g.* colostrum has a lower pH (6.3) than milk at
966 the end of lactation (McIntyre *et al*, 1952), and according to certain physio-pathological
967 conditions, *e.g.* when the animal suffers from mastitis the pH is higher (7.4) (Ziv *et al*, 1974).
968 Hence, to refine the PBPK model it would be useful to include the physiological variation of
969 milk pH over the different lactation and (patho)physiological stages.
970
971 4.3.3. Binding
972 Our PBPK model has the advantage of accounting for the distribution of OTC in milk
973 fat and aqueous phase, its binding to casein, whey protein, ionized magnesium, and calcium.
974 Because the composition of milk varies between species (Balthazar *et al*, 2017; Park *et al*,
975 2007) and that affinities differ between molecules, it is important to account for all major milk
976 components for future cross-species and cross-molecule extrapolations. The binding of OTC
977 to ionized cations was taken into consideration as this is a known characteristic of
978 tetracyclines (as for fluoroquinolones) (Ross and Riley, 1993) and since Ca^{2+} and Mg^{2+}
979 concentrations are high in milk. Somatic cell binding was neglected, because even in case of
980 serious mastitis (5 000 000 cells/ml), the volume of somatic cells represents less than 0.2% of
981 the milk volume (Campbell and Marshall, 2016). Furthermore, to the knowledge of the
982 authors of this study, no article mentions the binding of OTC to white blood cells.
983
984 The affinities of OTC for the milk components (*i.e.,* fat, casein, calcium, and
985 magnesium) were calculated using linear regressions constructed from experimental data
986 available in the literature for several drugs (Carlotti *et al*, 2012; Lupton *et al*, 2018; Shappell

et al, 2017). However, in case of extrapolation to other molecules, these data may not be available. Recently, Abduljalil *et al* (Abduljalil *et al*, 2021) proposed an approach to calculate the free fraction in milk (fu_{milk}) from the lipophilicity (logP) of a molecule. However, this approach would appear to have some limitations, as for OTC, which has a low logP (-4.54), the fu_{milk} value estimated using the formula of Abduljalil *et al* is higher than 1 (1.26 for both species).

According to this study model, OTC was predicted to be bound more in milk (~60%) than in plasma (~20%). OTC was predicted to be bound mainly to ionized calcium, ionized magnesium and lightly to whey proteins, so it was mainly within the skimmed milk. These findings could be interesting concerning milk by-products.

This PBPK model also takes into account the binding of OTC to different cellular components in the udder (*i.e.,* lipids and phospholipids). The partition coefficient of OTC between udder and plasma (k_{udder}, ratio of udder and plasma concentrations) was calculated to be 0.75 for cows and 0.77 for goats. It is of the same order of magnitude as those of other tissues (*i.e.,* muscle, liver, the rest) (see Table 1). As mentioned above, the binding in the udder IW resulted in drug retention and IW acted as a deep compartment. The slow release of the drug from the IW sub-compartment partly explains the delay of T_{max} in milk compared to plasma. This compartment could thus be useful for extrapolation to other molecules, especially those with strong IW binding.

4.3.4. Passive diffusion

The current PBPK model accounts for passive diffusion (CL_{diff}) between the udder and milk, calculated from *in vitro* permeability (Papp). Papp is a parameter that varies greatly between molecules (*e.g.* caffeine with a Papp of 10^{-5} cm/s; norfloxacin with a Papp of 10^{-7} cm/s (Chen *et al*, 2008) and amoxicillin with a Papp of 10^{-8} cm/s in an internal unpublished study). A lower value of Papp (10^{-8} cm/s) slows down the passage into milk (C_{max} of 0.43 mg/L at 19h *vs* 2.52 mg/L at 12h for a Papp of 10^{-7} cm/s) whereas a higher value of Papp (10^{-5} cm/s) increases the passage in the first hours after administration (C_{max} of 4.27 mg/L at 6h) (Figure 6). The low permeability of OTC (Papp = 1.4 x 10^{-7} cm/s) was responsible for the delay in appearance in milk (see Figure S6 and S7 in supplementary materials), but also for the slow release from the IW compartment that led to an increased elimination half-life in

1020 milk (7.9h). By simulating other values of Papp for the OTC, similar elimination half-life
1021 values for Papp of 10^{-5} cm/s and 10^{-6} cm/s (7.4 hours) and a value 30% higher for Papp of 10^{-8}
1022 cm/s (9.8 hours) would have ben obtained. Therefore, permeability might be of importance
1023 for generalizing the PBPK model to other molecules.

1024

1025 4.4. Differences between cows and goats

1026 As explained above, this generic PBPK model is intended to be used in cross-species
1027 extrapolation. It was able to satisfactorily predict milk concentrations of OTC for both cows
1028 and goats, but the predictions did not differ much between the two species. As the milk pH is
1029 almost identical between the two species (6.68 for cows and 6.65 for goats), the rate of
1030 ionization of OTC is identical in the milk of cows and goats. A key difference between cow
1031 and goat milk is the concentration of whey proteins (Balthazar *et al*, 2017), but as OTC has a
1032 low affinity for these proteins this difference has little impact on its binding in milk. OTC
1033 binds mainly to ionized calcium, which is in similar concentrations in both species (0.08 g/L
1034 for cows, 0.09 g/L for goats). Therefore, we did not predict any difference in the binding of
1035 OTC in milk between the two species. Finally, the main differences in milk excretion
1036 between the two species were explained by the differences in the plasma profile of OTC.

1037

1038 For other molecules with stronger affinities for milk components that vary between
1039 species, such as fat and protein, greater differences in milk concentrations could be observed.

1040

1041 4.5. Model application to estimate withdrawal period in milk

1042 For the estimation of WP in milk, a literature was performed for estimates of inter-
1043 individual variabilities (IIV) for the different parameters of the PBPK model. For some
1044 parameters the variability took into account the differences between animals of the same
1045 breed, for others it took into account the differences between breeds of the same species. For
1046 the few parameters without available experimental data, the fixed CV of 30% represents a
1047 moderate level of variability (Covington *et al*., 2007), while for chemical parameters, a CV of
1048 20% represents the uncertainty of these parameters values. These CV values are well
1049 accepted in the field of PBPK modelling and are often used in recently published papers
1050 (Clewell and Clewell, 2008; Henri *et al*, 2017a; Li *et al*, 2017, 2019a; Riad *et al*, 2021).

1051

For cows, the model-predicted WPs (rounded up to the next full day) were slightly higher than the labelled milk discard time for both standard dosing regimens, *i.e.*, five (5) days *vs* four (4) days after four (4) repeated IM injections of OTC 10 mg/kg and four (4) days *vs* three (3) days after three (3) repeated IM injections OTC 5 mg/kg. These WPs are highly dependent on the prediction intervals, which were based on the IIV and uncertainty of the model parameters. The latter may have been overestimated and resulted in slightly higher estimated WPs.

For goats, predicted WPs were consistent with the labelled milk discard time for both standard dosing regimens, *i.e.*, four (4) days after four (4) repeated IM injections of OTC 10 mg/kg and three (3) days after three (3) repeated IM injections OTC 5 mg/kg). Because total plasma clearance is higher in goats, plasma concentrations are lower and the time that residues fall below the established MRL is reduced compared to that of cows. This observation was also reported by Riad *et al* (Riad *et al*, 2021). In addition, for goats, the labelled WP of OTC have been fixed at the WP of cows (EMA, 2016) and do not take into account the physiology and particularities of the species. Thus, an experimental study would be necessary to confirm those predicted WP in goat milk.

Overall, the popPBPK model described in this study could be used as a tool to anticipate residue depletion studies. Such a model does not completely replace animal studies but it can help to design such studies.

4.6. PBPK model limitations

Although this generic model accurately predicted OTC concentrations in milk of both species, it has some limitations.

First, passive diffusion is the only mechanism of drug distribution in milk that was considered in the current model. Indeed, although OTC is known to be a substrate of PgP (Schrickx and Fink-Gremmels, 2007), the latter is under expressed in the udder during lactation and does not play a role in transporting the molecule into milk (Yagdiran *et al*, 2016). However, other transporters that are highly expressed in the udder or whose expression increases during lactation (García-Lino *et al*, 2019) may have an important role in

1084 the exchange of drugs (and nutrients) between plasma and milk (Mahnke *et al*, 2016;
1085 Ozdemir, 2018). Further studies will be conducted with other drugs to investigate the role of
1086 active transport of molecules in milk. An influx and/or efflux clearance could then be added
1087 to equations 8, 9, and 18.
1088
1089 Thus, the current model considers drug binding to milk components but does not vary
1090 the milk components concentrations over time, as observed in reality (Ciappesoni *et al*, 2011;
1091 Coulon *et al*, 1991). Further studies are needed to add variation over time of these parameters
1092 to this model. Similarly, changes in milk pH over time may be added to the model.
1093
1094 On the other hand, to build this population model variabilities and uncertainties on
1095 parameters (Balthazar *et al*, 2017; Craigmill *et al*, 2004, 2000; Lautz *et al*, 2020; Li *et al*,
1096 2021; Lin *et al*, 2020, 2016; Nouws *et al*, 1985b; Upton, 2008) were applied. The
1097 physiological data for cows and goats were mainly derived from two recent reviews of the
1098 literature (Li *et al*, 2021; Lin *et al*, 2020). These two reviews are compiled based on a number
1099 of original experimental studies and represent the most accurate physiological parameter data
1100 for these species in the literature. Thus, uncertainty has been substantially decreased for
1101 many physiological parameters, but some are still missing. On the other hand, the
1102 correlations between the different physiological values are not described and considering
1103 independent variabilities may lead to an overestimation of the overall variability. The choice
1104 of the random effects model is critical for the determination of WP with population PBPK
1105 models. However, there is no real consensus on how to predict WP from popPBPK models.
1106 Some authors consider that the 99th percentile of the PI obtained by a population model is a
1107 good approximation of the 95th percentile of the tolerance interval, which is the criterion used
1108 by regulatory agencies, and can therefore be used to predict a WP (Chevance, 2017; Henri *et*
1109 *al*, 2017b; Viel, 2018). In this study case, the internal and external validations that were
1110 carried out give an indication that the choice of the random model was reasonable. However,
1111 the choice was arbitrary and since it incorporates both IIV and parameter uncertainty it is
1112 difficult to determine whether the resulting interval was a prediction interval or a confidence
1113 interval.
1114
1115 4.7. Perspectives

In conclusion, the popPBPK model successfully predicted OTC concentrations in cow and goat milk after different doses and routes of administration. This is the first generic PBPK model to consider the udder as a permeability-limited compartment, accounting for vascular, EW, IW, alveolar, and cisternal spaces, as well as passive diffusion across physiological membranes, pH, ionization, and the composition of milk.

By integrating inter-individual variability in the physiological values into the model, and uncertainty in the parameters used, the model allowed for a suitable estimation of the WPs of OTC for cows and goats for different dosing regimens.

In the future, this model could be extrapolated to different drugs and chemicals, such as pesticides, with different affinities and physico-chemical properties, and to different species, such as sheep and humans, with a different milk composition and milk production.

Acknowledgements

This work was financially supported by the Nouvelle Aquitaine Region and the laboratory Ceva Animal Health. We would like to acknowledge Christophe Buffet, Balladyne Tritsch, Julian Laroche, Christophe Adier, Marie-Pierre Lagree, and Dominique Hurtaud-Pessel for their analytical support. We thank Emilie Wimmer, Denis Boulanger, Melaine Sauvee, Bertrand Minaud, Melanie Bouteille, Sylvie Ecalle, and Jeremy Roger, the team of the agricultural high schools of Melle and Venours, for the help in the realization of *in vivo* experimentations. We would additionally like to thank Thierry Vidard and Jean-Guy Rolland, for technical support.

References

Abduljalil, K., Pansari, A., Ning, J., Jamei, M., 2021. Prediction of drug concentrations in milk during breastfeeding, integrating predictive algorithms within a physiologically-based pharmacokinetic model. CPT: Pharmacometrics & Systems Pharmacology 10, 878–889. https://doi.org/10.1002/psp4.12662

Achenbach, T.E., 1995. Physiological and classical pharmacokinetic models of oxytetracycline in cattle 129.

Aktas, İ., Yarsan, E., 2017. Pharmacokinetics of Conventional and Long-Acting Oxytetracycline Preparations in Kilis Goat. Frontiers in Veterinary Science 4. https://doi.org/10.3389/fvets.2017.00229

1150 Alberghina, D., Casella, S., Vazzana, I., Ferrantelli, V., Giannetto, C., Piccione, G., 2010.
1151 Analysis of serum proteins in clinically healthy goats (Capra hircus) using agarose gel
1152 electrophoresis. Vet Clin Pathol 39, 317–321. https://doi.org/10.1111/j.1939-
1153 165X.2010.00226.x

1154 Ayadi, M., Caja, G., Such, X., Knight, C.H., 2003. Use of ultrasonography to estimate cistern
1155 size and milk storage at different milking intervals in the udder of dairy cows. J. Dairy
1156 Res. 70, 1–7. https://doi.org/10.1017/s0022029902005873

1157 Badhan, R.K.S., Chenel, M., Penny, J.I., 2014. Development of a Physiologically-Based
1158 Pharmacokinetic Model of the Rat Central Nervous System. Pharmaceutics 6, 97–136.
1159 https://doi.org/10.3390/pharmaceutics6010097

1160 Balthazar, C.F., Pimentel, T.C., Ferrão, L.L., Almada, C.N., Santillo, A., Albenzio, M.,
1161 Mollakhalili, N., Mortazavian, A.M., Nascimento, J.S., Silva, M.C., Freitas, M.Q.,
1162 Sant'Ana, A.S., Granato, D., Cruz, A.G., 2017. Sheep Milk: Physicochemical
1163 Characteristics and Relevance for Functional Food Development. Comprehensive
1164 Reviews in Food Science and Food Safety 16, 247–262. https://doi.org/10.1111/1541-
1165 4337.12250

1166 Beal, S.L., 2001. Ways to Fit a PK Model with Some Data Below the Quantification Limit. J
1167 Pharmacokinet Pharmacodyn 28, 481–504. https://doi.org/10.1023/A:1012299115260

1168 Bobbo, T., Fiore, E., Gianesella, M., Morgante, M., Gallo, L., Ruegg, P.L., Bittante, G.,
1169 Cecchinato, A., 2017. Variation in blood serum proteins and association with somatic
1170 cell count in dairy cattle from multi-breed herds. Animal 11, 2309–2319.
1171 https://doi.org/10.1017/S1751731117001227

1172 Caja, G., Ayadi, M., Knight, C.H., 2004. Changes in cisternal compartment based on stage of
1173 lactation and time since milk ejection in the udder of dairy cows. J. Dairy Sci. 87,
1174 2409–2415. https://doi.org/10.3168/jds.S0022-0302(04)73363-9

1175 Campbell, J.R., Marshall, R.T., 2016. Dairy Production and Processing: The Science of Milk
1176 and Milk Products. Waveland Press.

1177 Carlotti, B., Cesaretti, A., Elisei, F., 2012. Complexes of tetracyclines with divalent metal
1178 cations investigated by stationary and femtosecond-pulsed techniques. Phys. Chem.
1179 Chem. Phys. 14, 823–834. https://doi.org/10.1039/C1CP22703C

1180 Chemicalize - Instant Cheminformatics Solutions [WWW Document], n.d. URL
1181 https://chemicalize.com/app/calculation/oxytetracycline (accessed 1.29.21).

1182 Chen, X., Murawski, A., Patel, K., Crespi, C.L., Balimane, P.V., 2008. A novel design of
1183 artificial membrane for improving the PAMPA model. Pharm Res 25, 1511–1520.
1184 https://doi.org/10.1007/s11095-007-9517-8

1185 Cheng, Y.-H., Lin, Y.-J., You, S.-H., Yang, Y.-F., How, C.M., Tseng, Y.-T., Chen, W.-Y.,
1186 Liao, C.-M., 2016. Assessing exposure risks for freshwater tilapia species posed by
1187 mercury and methylmercury. Ecotoxicology 25, 1181–1193.
1188 https://doi.org/10.1007/s10646-016-1672-4

1189 Chevance, 2017. The present and future of withdrawal period calculations for milk in the
1190 European Union: focus on heterogeneous, nonmonotonic data - Chevance - 2017 -
1191 Journal of Veterinary Pharmacology and Therapeutics - Wiley Online Library [WWW
1192 Document]. URL https://onlinelibrary.wiley.com/doi/abs/10.1111/jvp.12351 (accessed
1193 11.8.19).

Ciappesoni, G., JPřibyl, Milerski, M., Mareš, V., 2011. Factors affecting goat milk yield and its composition. Czech Journal of Animal Science 49, 465–473. https://doi.org/10.17221/4333-CJAS

Clewell, R.A., Clewell, H.J., 2008. Development and specification of physiologically based pharmacokinetic models for use in risk assessment. Regulatory Toxicology and Pharmacology 50, 129–143. https://doi.org/10.1016/j.yrtph.2007.10.012

Coulon, J.B., CHILLIARD, Y., Rémond, B., 1991. Effets du stade physiologique et de la saison sur la composition chimique du lait de vache et ses caractéristiques technologiques (aptitude à la coagulation, lipolyse). INRA Productions Animales 4, 219–228.

Covington, T.R., Robinan Gentry, P., Van Landingham, C.B., Andersen, M.E., Kester, J.E., Clewell, H.J., 2007. The use of Markov chain Monte Carlo uncertainty analysis to support a Public Health Goal for perchloroethylene. Regulatory Toxicology and Pharmacology 47, 1–18. https://doi.org/10.1016/j.yrtph.2006.06.008

Craigmill, A.L., 2003. A physiologically based pharmacokinetic model for oxytetracycline residues in sheep. Journal of Veterinary Pharmacology and Therapeutics 26, 55–63. https://doi.org/10.1046/j.1365-2885.2003.00451.x

Craigmill, A.L., Holland, R.E., Robinson, D., Wetzlich, S., Arndt, T., 2000. Serum pharmacokinetics of oxytetracycline in sheep and calves and tissue residues in sheep following a single intramuscular injection of a long-acting preparation. J. Vet. Pharmacol. Ther. 23, 345–352.

Craigmill, A.L., Miller, G.R., Gehring, R., Pierce, A.N., Riviere, J.E., 2004. Meta-analysis of pharmacokinetic data of veterinary drugs using the Food Animal Residue Avoidance Databank: oxytetracycline and procaine penicillin G. J. Vet. Pharmacol. Ther. 27, 343–353. https://doi.org/10.1111/j.1365-2885.2004.00606.x

EMA, 2016. Guideline on safety and residue data requirements for pharmaceutical veterinary medicinal products intended for minor use or minor species (MUMS)/limited market 26.

Fenneteau, F., Li, J., Nekka, F., 2009. Assessing drug distribution in tissues expressing P-glycoprotein using physiologically based pharmacokinetic modeling: identification of important model parameters through global sensitivity analysis. J Pharmacokinet Pharmacodyn 36, 495. https://doi.org/10.1007/s10928-009-9134-8

Fisher, J.W., Gearhart, J.M., Lin, Z. (Eds.), 2020. Physiologically Based Pharmacokinetic (PBPK) Modeling. Academic Press. https://doi.org/10.1016/B978-0-12-818596-4.00013-8

Fujikawa, M., Ano, R., Nakao, K., Shimizu, R., Akamatsu, M., 2005. Relationships between structure and high-throughput screening permeability of diverse drugs with artificial membranes: Application to prediction of Caco-2 cell permeability. Bioorganic & Medicinal Chemistry 13, 4721–4732. https://doi.org/10.1016/j.bmc.2005.04.076

García-Lino, A.M., Álvarez-Fernández, I., Blanco-Paniagua, E., Merino, G., Álvarez, A.I., 2019. Transporters in the Mammary Gland-Contribution to Presence of Nutrients and Drugs into Milk. Nutrients 11. https://doi.org/10.3390/nu11102372

Henri, J., Carrez, R., Méda, B., Laurentie, M., Sanders, P., 2017a. A physiologically based pharmacokinetic model for chickens exposed to feed supplemented with monensin

during their lifetime. Journal of Veterinary Pharmacology and Therapeutics 40, 370–382. https://doi.org/10.1111/jvp.12370

Henri, J., Jacques, A.-M., Sanders, P., Chevance, A., Laurentie, M., 2017b. The present and future of withdrawal period calculations for milk in the European Union: dealing with data below the limit of quantification. J. Vet. Pharmacol. Ther. 40, 116–122. https://doi.org/10.1111/jvp.12343

Hotham, N., Hotham, E., 2015. Drugs in breastfeeding. Aust Prescr 38, 156–159. https://doi.org/10.18773/austprescr.2015.056

Jackson, P.G., Cockcroft, P.D., 2002. Clinical Examination of Farm Animals. Blackwell Science.

Jamei, M., Bajot, F., Neuhoff, S., Barter, Z., Yang, J., Rostami-Hodjegan, A., Rowland-Yeo, K., 2014. A Mechanistic Framework for In Vitro–In Vivo Extrapolation of Liver Membrane Transporters: Prediction of Drug–Drug Interaction Between Rosuvastatin and Cyclosporine. Clin Pharmacokinet 53, 73–87. https://doi.org/10.1007/s40262-013-0097-y

Jarrett, A.M., Gao, Y., Hussaini, M.Y., Cogan, N.G., Katz, D.F., 2016. Sensitivity Analysis of a Pharmacokinetic Model of Vaginal Anti-HIV Microbicide Drug Delivery. J Pharm Sci 105, 1772–1778. https://doi.org/10.1016/j.xphs.2016.02.015

Ji, S.K., Zhang, F., Sun, Y., Deng, K., Wang, B., Tu, Y., Zhang, N.F., Jiang, C.G., Wang, S., Diao, Q.-Y., 2017. Influence of dietary slow-release urea on growth performance, organ development and serum biochemical parameters of mutton sheep. Journal of animal physiology and animal nutrition. https://doi.org/10.1111/jpn.12532

Kansy, M., Senner, F., Gubernator, K., 1998. Physicochemical high throughput screening: parallel artificial membrane permeation assay in the description of passive absorption processes. J Med Chem 41, 1007–1010. https://doi.org/10.1021/jm970530e

Kinsella, J.E., McCarthy, R.D., 1968. Lipid composition and secretory activity of bovine mammary cells in vitro. Biochim. Biophys. Acta 164, 530–539. https://doi.org/10.1016/0005-2760(68)90182-3

Konar, A., Thomas, P.C., K.g, T., 1972. The composition of ovine mammary cells. Comparative Biochemistry and Physiology Part A: Physiology 41, 195–203. https://doi.org/10.1016/0300-9629(72)90047-3

Larson, B., 1978. The Mammary Gland/Human Lactation/Milk Synthesis. Elsevier. https://doi.org/10.1016/C2013-0-11043-4

Lautz, L.S., Dorne, J.L.C.M., Oldenkamp, R., Hendriks, A.J., Ragas, A.M.J., 2020. Generic physiologically based kinetic modelling for farm animals: Part I. Data collection of physiological parameters in swine, cattle and sheep. Toxicology Letters 319, 95–101. https://doi.org/10.1016/j.toxlet.2019.10.021

Lautz, L.S., Oldenkamp, R., Dorne, J.L., Ragas, A.M.J., 2019. Physiologically based kinetic models for farm animals: Critical review of published models and future perspectives for their use in chemical risk assessment. Toxicology in Vitro 60, 61–70. https://doi.org/10.1016/j.tiv.2019.05.002

Law, F.C.P., 1999. A Physiologically Based Pharmacokinetic Model for Predicting the Withdrawal Period of Oxytetracycline in Cultured Chinook Salmon (Oncorhynchus Tshawytscha), in: Smith, D.J., Gingerich, W.H., Beconi-Barker, M.G. (Eds.),

Xenobiotics in Fish. Springer US, Boston, MA, pp. 105–121. https://doi.org/10.1007/978-1-4615-4703-7_8

Leavens, T.L., Tell, L.A., Kissell, L.W., Smith, G.W., Smith, D.J., Wagner, S.A., Shelver, W.L., Wu, H., Baynes, R.E., Riviere, J.E., 2014. Development of a physiologically based pharmacokinetic model for flunixin in cattle (Bos taurus). Food Additives & Contaminants: Part A 31, 1506–1521. https://doi.org/10.1080/19440049.2014.938363

Leitner, G., Merin, U., Silanikove, N., 2004. Changes in Milk Composition as Affected by Subclinical Mastitis in Goats. Journal of dairy science 87, 1719–26. https://doi.org/10.3168/jds.S0022-0302(04)73325-1

Li, M., Cheng, Y.-H., Chittenden, J.T., Baynes, R.E., Tell, L.A., Davis, J.L., Vickroy, T.W., Riviere, J.E., Lin, Z., 2019a. Integration of Food Animal Residue Avoidance Databank (FARAD) empirical methods for drug withdrawal interval determination with a mechanistic population-based interactive physiologically based pharmacokinetic (iPBPK) modeling platform: example for flunixin meglumine administration. Arch Toxicol. https://doi.org/10.1007/s00204-019-02464-z

Li, M., Gehring, R., Riviere, J.E., Lin, Z., 2018. Probabilistic Physiologically Based Pharmacokinetic Model for Penicillin G in Milk From Dairy Cows Following Intramammary or Intramuscular Administrations. Toxicological Sciences 164, 85–100. https://doi.org/10.1093/toxsci/kfy067

Li, M., Gehring, R., Riviere, J.E., Lin, Z., 2017. Development and application of a population physiologically based pharmacokinetic model for penicillin G in swine and cattle for food safety assessment. Food Chem. Toxicol. 107, 74–87. https://doi.org/10.1016/j.fct.2017.06.023

Li, M., Mainquist-Whigham, C., Karriker, L.A., Wulf, L.W., Zeng, D., Gehring, R., Riviere, J.E., Coetzee, J.F., Lin, Z., 2019b. An integrated experimental and physiologically based pharmacokinetic modeling study of penicillin G in heavy sows. Journal of Veterinary Pharmacology and Therapeutics 0. https://doi.org/10.1111/jvp.12766

Li, M., Wang, Y.-S., Elwell-Cuddy, T., Baynes, R.E., Tell, L.A., Davis, J.L., Maunsell, F.P., Riviere, J.E., Lin, Z., 2021. Physiological parameter values for physiologically based pharmacokinetic models in food-producing animals. Part III: Sheep and goat. J Vet Pharmacol Ther 44, 456–477. https://doi.org/10.1111/jvp.12938

Lin, Z., Gehring, R., Mochel, J.P., Lavé, T., Riviere, J.E., 2016. Mathematical modeling and simulation in animal health - Part II: principles, methods, applications, and value of physiologically based pharmacokinetic modeling in veterinary medicine and food safety assessment. J. Vet. Pharmacol. Ther. 39, 421–438. https://doi.org/10.1111/jvp.12311

Lin, Z., Li, M., Gehring, R., Riviere, J.E., 2015. Development and application of a multiroute physiologically based pharmacokinetic model for oxytetracycline in dogs and humans. J Pharm Sci 104, 233–243. https://doi.org/10.1002/jps.24244

Lin, Z., Li, M., Wang, Y.-S., Tell, L.A., Baynes, R.E., Davis, J.L., Vickroy, T.W., Riviere, J.E., 2020. Physiological parameter values for physiologically based pharmacokinetic models in food-producing animals. Part I: Cattle and swine. Journal of Veterinary Pharmacology and Therapeutics n/a. https://doi.org/10.1111/jvp.12861

Lupton, S.J., Shappell, N.W., Shelver, W.L., Hakk, H., 2018. Distribution of Spiked Drugs between Milk Fat, Skim Milk, Whey, Curd, and Milk Protein Fractions: Expansion of

Partitioning Models. J. Agric. Food Chem. 66, 306–314. https://doi.org/10.1021/acs.jafc.7b04463

Mahnke, H., Ballent, M., Baumann, S., Imperiale, F., von Bergen, M., Lanusse, C., Lifschitz, A.L., Honscha, W., Halwachs, S., 2016. The ABCG2 Efflux Transporter in the Mammary Gland Mediates Veterinary Drug Secretion across the Blood-Milk Barrier into Milk of Dairy Cows. Drug Metabolism and Disposition 44, 700–708. https://doi.org/10.1124/dmd.115.068940

Maltz, E., Blatchford, D.R., Peaker, M., 1984. Effects of Frequent Milking on Milk Secretion and Mammary Blood Flow in the Goat. Quarterly Journal of Experimental Physiology 69, 127–132. https://doi.org/10.1113/expphysiol.1984.sp002773

Martens, H., Stumpff, F., 2019. Assessment of magnesium intake according to requirement in dairy cows. Journal of Animal Physiology and Animal Nutrition 103, 1023–1029. https://doi.org/10.1111/jpn.13106

McCutcheon, S.N., Blair, H.T., Purchas, R.W., 1993. Body composition and organ weights in fleeceweight-selected and control Romney rams. New Zealand Journal of Agricultural Research 36, 445–449. https://doi.org/10.1080/00288233.1993.10417745

McIntyre, R.T., Parrish, D.B., Fountaine, F.C., 1952. Properties of the Colostrum of the Dairy Cow. VII. pH, Buffer Capacity and Osmotic Pressure1. Journal of Dairy Science 35, 356–362. https://doi.org/10.3168/jds.S0022-0302(52)93714-4

Mevius, D.J., Vellenga, L., Breukink, H.J., Nouws, J.F., Vree, T.B., Driessens, F., 1986. Pharmacokinetics and renal clearance of oxytetracycline in piglets following intravenous and oral administration. Vet Q 8, 274–284. https://doi.org/10.1080/01652176.1986.9694056

Nestorov, I.A., Aarons, L.J., Arundel, P.A., Rowland, M., 1998. Lumping of whole-body physiologically based pharmacokinetic models. J Pharmacokinet Biopharm 26, 21–46. https://doi.org/10.1023/a:1023272707390

Neville, M.C., Watters, C.D., 1983. Secretion of Calcium into Milk: Review. Journal of Dairy Science 66, 371–380. https://doi.org/10.3168/jds.S0022-0302(83)81802-5

Ng, C.A., Hungerbühler, K., 2013. Bioconcentration of Perfluorinated Alkyl Acids: How Important Is Specific Binding? Environ. Sci. Technol. 47, 7214–7223. https://doi.org/10.1021/es400981a

Nouws, J.F.M., Breukink, H.J., Binkhorse, G.J., Lohuis, J., van Lith, P., Mevius, D.J., Vree, T.B., 1985a. Comparative pharmacokinetics and bioavailability of eight parenteral oxytetracycline-10% formulations in dairy cows. Veterinary Quarterly 7, 306–314. https://doi.org/10.1080/01652176.1985.9694004

Nouws, J.F.M., Vree, T.B., Termond, E., Lohuis, J., van Lith, P., Binkhorst, G.J., Breukink, H.J., 1985b. Pharmacokinetics and renal clearance of oxytetracycline after intravenous and intramuscular administration to dairy cows. Veterinary Quarterly 7, 296–305. https://doi.org/10.1080/01652176.1985.9694003

Oh, H., Deeth, H., 2017. Magnesium in milk. International Dairy Journal 71. https://doi.org/10.1016/j.idairyj.2017.03.009

Ozdemir, Z., 2018. Behaviours of Drugs in the Milk -A Review. Atatürk Üniversitesi Vet. Bil. Derg.

Park, Y.W., Juárez, M., Ramos, M., Haenlein, G.F.W., 2007. Physico-chemical characteristics of goat and sheep milk. Small Ruminant Research, Special Issue: Goat and Sheep Milk 68, 88–113. https://doi.org/10.1016/j.smallrumres.2006.09.013

Peaker, M., Blatchford, D.R., 1988. Distribution of milk in the goat mammary gland and its relation to the rate and control of milk secretion. Journal of Dairy Research 55, 41–48. https://doi.org/10.1017/S0022029900025838

Peters, S.A., 2012. Physiologically-Based Modeling, in: Physiologically-Based Pharmacokinetic (PBPK) Modeling and Simulations. John Wiley & Sons, Ltd, pp. 13–16. https://doi.org/10.1002/9781118140291.ch2

Prosser, 1996. Regulation of Blood Flow in the Mammary Microvasculature. Journal of Dairy Science 79, 1184–1197. https://doi.org/10.3168/jds.S0022-0302(96)76472-X

Reijenga, J., van Hoof, A., van Loon, A., Teunissen, B., 2013. Development of Methods for the Determination of pKa Values. Anal Chem Insights 8, 53–71. https://doi.org/10.4137/ACI.S12304

Riad, M.H., Baynes, R.E., Tell, L.A., Davis, J.L., Maunsell, F.P., Riviere, J.E., Lin, Z., 2021. Development and Application of an Interactive Physiologically Based Pharmacokinetic (iPBPK) Model to Predict Oxytetracycline Tissue Distribution and Withdrawal Intervals in Market-Age Sheep and Goats. Toxicological Sciences 183, 253–268. https://doi.org/10.1093/toxsci/kfab095

Rodgers, T., Leahy, D., Rowland, M., 2005. Physiologically based pharmacokinetic modeling 1: predicting the tissue distribution of moderate-to-strong bases. J Pharm Sci 94, 1259–1276. https://doi.org/10.1002/jps.20322

Rodgers, T., Rowland, M., 2006. Physiologically based pharmacokinetic modelling 2: predicting the tissue distribution of acids, very weak bases, neutrals and zwitterions. J Pharm Sci 95, 1238–1257. https://doi.org/10.1002/jps.20502

Ross, D.L., Riley, C.M., 1993. Physicochemical properties of the fluoroquinolone antimicrobials V. Effect of fluoroquinolone structure and pH on the complexation of various fluoroquinolones with magnesium and calcium ions. International Journal of Pharmaceutics 93, 121–129. https://doi.org/10.1016/0378-5173(93)90170-K

Rule, R., Moreno, L., Serrano, J., Roman, A.G., Moyano, R., Garcia, J., 2001. Pharmacokinetics and residues in milk of oxytetra-cyclines administered parenterally to dairy goats. Australian Veterinary Journal 79, 492–496. https://doi.org/10.1111/j.1751-0813.2001.tb13023.x

Saltelli, A., Bolado, R., 1998. An alternative way to compute Fourier amplitude sensitivity test (FAST). Computational Statistics & Data Analysis 26, 445–460. https://doi.org/10.1016/S0167-9473(97)00043-1

Schrickx, J., Fink-Gremmels, J., 2007. P-glycoprotein-mediated transport of oxytetracycline in the Caco-2 cell model. J. Vet. Pharmacol. Ther. 30, 25–31. https://doi.org/10.1111/j.1365-2885.2007.00808.x

Shanler, M.S., Mason, A.K., Crocker, R.M., Vardaro, R., Crespi, C.L., Stresser, D.M., Perloff, E.S., 2021. Automation of Corning® BioCoat™ Pre-coated PAMPA Plates Improves Predictability, Reproducibility, and Efficiency 5.

Shappell, N., Shelver, W., Lupton, S., Fanaselle, W., Doren, J., Hakk, H., 2017. Distribution of Animal Drugs among Curd, Whey, and Milk Protein Fractions in Spiked Skim Milk

and Whey. Journal of Agricultural and Food Chemistry 65. https://doi.org/10.1021/acs.jafc.6b04258

Snipes, M.B., Lengemann, F.W., 1972. Tissue Composition of Lactating Guinea Pia Mammary Glands. Journal of Dairy Science 55, 1783–1786. https://doi.org/10.3168/jds.S0022-0302(72)85758-8

Stephens, C.R., Murai, K., Brunings, K.J., Woodward, R.B., 1956. Acidity Constants of the Tetracycline Antibiotics. J. Am. Chem. Soc. 78, 4155–4158. https://doi.org/10.1021/ja01597a081

Szegezdi, J., Csizmadia, F., 2007. A method for calculating the pKa values of small and large molecules.

Szegezdi, J., Csizmadia, F., 2004. Prediction of dissociation co...

Thompson, G.E., 1980. The distribution of blood flow in the udder of the sheep and changes brought about by cold exposure and lactation. J Physiol 302, 379–386.

Tongaree, S., Flanagan, D.R., Poust, R.I., 1999. The Effects of pH and Mixed Solvent Systems on the Solubility of Oxytetracycline. Pharmaceutical Development and Technology 4, 571–580. https://doi.org/10.1081/PDT-100101396

Upton, R.N., 2008. Organ weights and blood flows of sheep and pig for physiological pharmacokinetic modelling. J Pharmacol Toxicol Methods 58, 198–205. https://doi.org/10.1016/j.vascn.2008.08.001

Vestweber, J.G., Al-Ani, F.K., 1984. Udder edema: biochemical studies in Holstein cattle. Cornell Vet 74, 366–372.

Viel, A., 2018. A Population WB-PBPK Model of Colistin and its Prodrug CMS in Pigs: Focus on the Renal Distribution and Excretion | SpringerLink [WWW Document]. URL https://link.springer.com/article/10.1007%2Fs11095-018-2379-4 (accessed 1.15.19).

Waddell, W.J., Bates, R.G., 1969. Intracellular pH. Physiol Rev 49, 285–329. https://doi.org/10.1152/physrev.1969.49.2.285

Whittem, T., 2012. Modelling the concentration–time relationship in milk from cattle administered an intramammary drug. Journal of Veterinary Pharmacology and Therapeutics 35, 460–471. https://doi.org/10.1111/j.1365-2885.2011.01352.x

WHO, 2010. Characterization and application of physiologically based pharmacokinetic models in risk assessment, Harmonization project document. World Health Organization, Geneva.

Williams, P., Kurlak, L., Perkins, A., Budge, H., Stephenson, T., Keisler, D., Symonds, M., Gardner, D., 2007. Hypertension and impaired renal function accompany juvenile obesity: The effect of prenatal diet. Kidney international 72, 279–89. https://doi.org/10.1038/sj.ki.5002276

Woodward, A.P., Whittem, T., 2019. Physiologically based modelling of the pharmacokinetics of three beta-lactam antibiotics after intra-mammary administration in dairy cows. J. Vet. Pharmacol. Ther. https://doi.org/10.1111/jvp.12812

Yagdiran, Y., Oskarsson, A., Knight, C.H., Tallkvist, J., 2016. ABC- and SLC-Transporters in Murine and Bovine Mammary Epithelium - Effects of Prochloraz. PLOS ONE 11, e0151904. https://doi.org/10.1371/journal.pone.0151904

Yau, E., Olivares-Morales, A., Gertz, M., Parrott, N., Darwich, A.S., Aarons, L., Ogungbenro, K., 2020. Global Sensitivity Analysis of the Rodgers and Rowland Model for Prediction of Tissue: Plasma Partitioning Coefficients: Assessment of the Key Physiological and Physicochemical Factors That Determine Small-Molecule Tissue Distribution. AAPS J 22, 41. https://doi.org/10.1208/s12248-020-0418-7

Ziv, G., Bogin, E., Shani, J., G. Sulman, F., 1974. Penetration of radioactive-labeled antibiotics from blood serum into milk in normal and mastitic ewes. Annales de Recherches Vétérinaires 5, 15–28.

Ziv, G., Sulman, F.G., 1975. Absorption of antibiotics by the bovine udder. J. Dairy Sci. 58, 1637–1644. https://doi.org/10.3168/jds.S0022-0302(75)84762-X

Ziv, G., Sulman, F.G., 1972. Binding of Antibiotics to Bovine and Ovine Serum. Antimicrobial Agents and Chemotherapy 2, 206–213. https://doi.org/10.1128/AAC.2.3.206

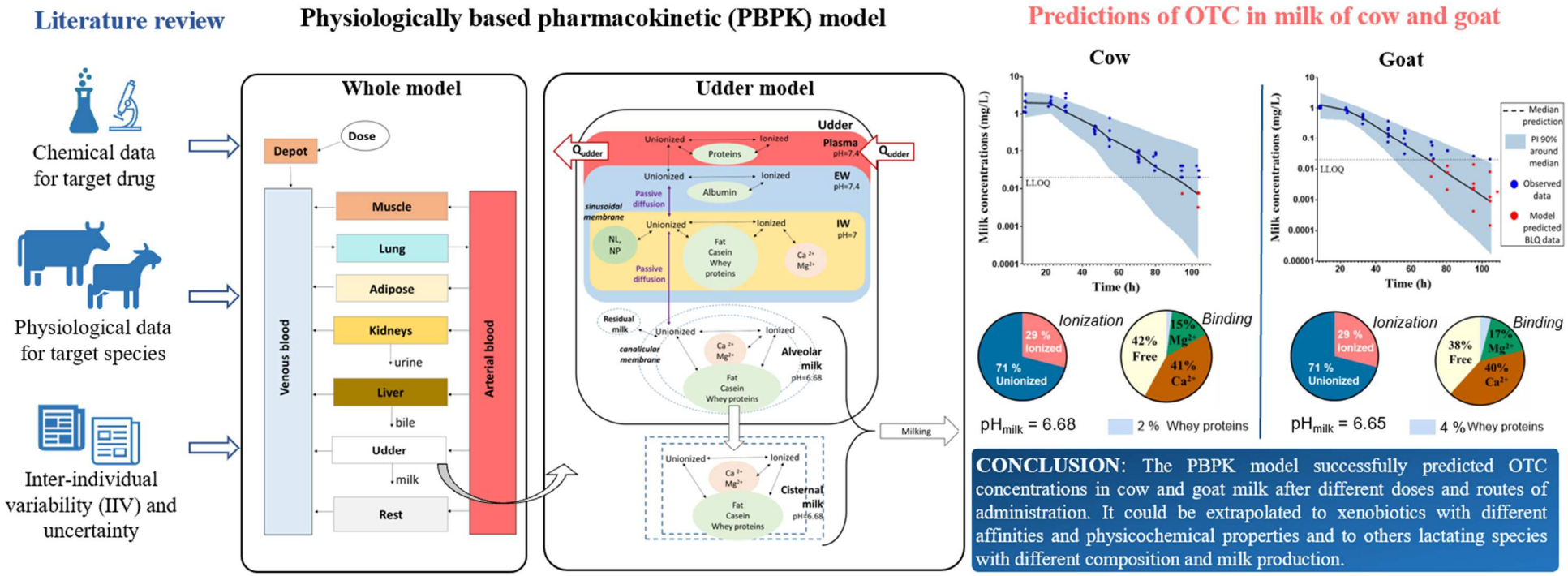
Literature review
Physiologically based pharmacokinetic (PBPK) model
Predictions of OTC in milk of cow and goat
Chemical data for target drug
Physiological data for target species
Inter-individual variability (IIV) and uncertainty
Whole model
Depot
Dose
Venous blood
Arterial blood
Muscle
Lung
Adipose
Kidneys
urine
Liver
bile
Udder
milk
Rest
Udder model
Udder
Plasma
pH=7.4
Proteins
EW
Albumin
IW
pH=7
sinusoidal membrane
Passive diffusion
NL, NP
Fat
Casein
Whey proteins
Residual milk
canalicular membrane
Alveolar milk
pH=6.68
Cisternal milk
Milking
Cow
Goat
Milk concentrations (mg/L)
Time (h)
LLOQ
Median prediction
PI 90% around median
Observed data
Model predicted BLQ data
Ionization
Binding
29 % Ionized
71 % Unionized
42% Free
15% Mg2+
41% Ca2+
38% Free
17% Mg2+
40% Ca2+
pHmilk = 6.68
2 % Whey proteins
pHmilk = 6.65
4 % Whey proteins
CONCLUSION: The PBPK model successfully predicted OTC concentrations in cow and goat milk after different doses and routes of administration. It could be extrapolated to xenobiotics with different affinities and physicochemical properties and to others lactating species with different composition and milk production.